

Received 17 June 2025, accepted 18 July 2025, date of publication 22 July 2025, date of current version 30 July 2025.

Digital Object Identifier 10.1109/ACCESS.2025.3591622

 SURVEY

Advances in Liver Tumour Diagnosis and Treatment: Etiology, Classification, and the Emerging Role of Machine Learning

YANA GAUR^{ID1}, ABHAY CHAUDHARY^{ID1}, AND AJITH ABRAHAM^{ID2,3}, (Senior Member, IEEE)

¹School of Computer Science and Engineering, Bennett University, Noida 201310, India

²School of Artificial Intelligence, Sai University, Chennai 603104, India

³Research Center, Artificial Intelligence Institute, Innopolis University, 420500 Innopolis, Russia

Corresponding authors: Yana Gaur (yanagaur2003@gmail.com) and Ajith Abraham (abraham.ajith@gmail.com)

This work was supported by the Ministry of Economic Development of Russian Federation, in June 2025, under Agreement 139-10-2025-034 and Agreement IGK 000000C313925P4D0002.

ABSTRACT Liver Tumours represent a significant global health challenge due to their diverse etiology, complex classification, and high mortality rates. This literature offers a comprehensive review of advancements in the diagnosis and treatment of liver tumours, encompassing their causes, classifications, symptoms, staging, and current treatment modalities. It begins with an exploration of the etiology and risk factors contributing to liver tumours, including genetic, environmental, and lifestyle influences, and a detailed classification into benign and malignant tumours. Staging systems, particularly the Barcelona Clinic Liver Cancer system, are discussed to elucidate diagnostic pathways and therapeutic implications. The paper delves into various treatment options, ranging from surgical approaches and locoregional therapies to systemic treatments such as targeted therapies and immunotherapies. Emerging treatment strategies, including the combination of Stereotactic Body Radiotherapy and immunotherapy, are highlighted for their potential to enhance survival outcomes. Additionally, significant attention is given to the transformative role of Artificial Intelligence in liver tumour diagnosis and treatment. This includes Artificial Intelligence applications in imaging modalities like Computed Tomography and Magnetic Resonance Imaging for segmentation, histopathological analysis, and predictive modeling for tumour growth and survival. The review also explores architectures such as Convolutional Neural Networks, U-Net and its variants, and Transformer-based models, which have been pivotal in segmentation, classification and prognosis. Furthermore, it discusses annotation tools that streamline dataset preparation, ensuring accurate and efficient training of Artificial Intelligence models. By providing a comprehensive analysis of existing literature and advancements, this review aims to support researchers and practitioners in advancing the field of liver tumour diagnosis and treatment.

INDEX TERMS Liver tumours, hepatocellular carcinoma, tumour classification, tumour staging, risk factors, treatment modalities, artificial intelligence, medical imaging, tumour growth prediction, diagnostic accuracy.

I. INTRODUCTION

Liver Tumours acts as a Consequential global health concern because of its diverse range of benign and malignant variations [1], [2], each with various sub-classifications.

The associate editor coordinating the review of this manuscript and approving it for publication was Gustavo Callico^{ID}.

These tumours show very different behaviours, treatment responses, and prognoses, and so it is necessary to have a comprehensive understanding of each of them, for effective management and right treatment to have improved patient outcomes [3]. It accounts for more than 8.3 per cent of global cancer deaths each year, these tumours are very hard to beat — especially in regions with high hepatitis B and C

prevalence such as East Asia and parts of Sub-Saharan Africa. The liver tumours have multifactorial etiology including chronic viral infection, alcohol-induced cirrhosis and rising epidemic of non-alcoholic fatty liver disease. Other than these, the development and progression of Liver tumours are also caused by genetic mutation and epigenetic alterations.

Liver tumours have a substantial economic burden with annual treatment costs in excess of \$1.6 billion in the United States and considerably more in resource-constrained settings where access to early diagnostic tools and therapies is limited. Improved early detection has benefited from recent diagnostic imaging such as dynamic contrast-enhanced MRI and biomarkers like alpha-fetoprotein. In addition, there are also new hope of targeted therapy and immunotherapy in advanced stage patients.

Thanks to artificial intelligence, the field is being revolutionized, in terms of precisely segmenting, staging and modelling tumor. These technologies will improve diagnostic accuracy and accelerate personalized treatment planning. As liver tumours present in variable ways and have a variable prognosis, it is essential to collaborate globally to overcome the pressing health care challenge by combining epidemiology, biology and AI driven technology.

A. ABBREVIATIONS AND ACRONYMS

The abbreviations used in this paper include imaging modalities such as **CT** (Computed Tomography). Surgical approaches include **ALPPS** (Associating Liver Partition and Portal vein Ligation for Staged Hepatectomy), aimed at improving resection outcomes. Diagnostic performance is often assessed using metrics like **AUC-ROC** (Area Under the Curve - Receiver Operating Characteristic), while Imaging modalities such as **DW-MRI** (Diffusion-Weighted Magnetic Resonance Imaging) provide critical insights into liver tumor characteristics. Specialized imaging techniques such as computed tomography arterial portography (**CTAP**) are used to enhance the visualization of liver vasculature and detect liver tumours with higher sensitivity. Conditions like **NAFLD** (Non-Alcoholic Fatty Liver Disease) and its progression to **NASH** (Non-Alcoholic Steatohepatitis) are significant risk factors. Primary liver cancer (**PLC**), which includes common types such as **HCC** (Hepatocellular Carcinoma), **HB** (Hepatoblastoma), and **CC** (Cholangiocarcinoma), presents with distinct histopathologic growth patterns (**HGP**). Hepatoblastoma (**HB**) is the most common pediatric liver cancer, characterized by its embryonal and fetal histological subtypes. Cholangiocarcinoma (**CC**) can be further classified into subtypes such as intrahepatic cholangiocarcinoma (**iCCA**), which originates within the liver. Additionally, secondary liver malignancies, such as **CRLM** (Colorectal Liver Metastases), represent a significant portion of liver tumor cases and require distinct treatment strategies. Risk factors such as prolonged use of **OCPs** (Oral Contraceptive Pills) have been associated with an increased risk of liver tumours. Treatment options range from locoregional therapies like **RFA** (Radiofrequency Ablation),

TACE (Transarterial Chemoembolization), **TARE** (Transarterial Radioembolization), and **PEI** (Percutaneous Ethanol Injection) to advanced interventions such as **SBRT** (Stereotactic Body Radiotherapy). Clinical outcomes are evaluated using measures such as **TOP** (Time of Progression), **OS** (Overall Survival), and **ORR** (Overall Response Rate), which provide insight into disease progression and treatment efficacy. Tumor mutational burden (**TMB**) is an emerging biomarker used to predict response to immunotherapy in liver cancer patients. Preclinical models such as patient-derived xenografts (**PDX**) play a crucial role in translational research by enabling personalized therapeutic testing and understanding tumor heterogeneity. Histopathological analysis utilizes digital pathology techniques such as whole slide imaging (**WSI**), **TMA** (Tissue Microarray) are employed to delineate tumor regions in medical images, improving diagnostic precision. Datasets like **LiTS** (Liver Tumor Segmentation) and **PAIP** (Pathology AI Platform) support AI-based advancements in pathology. AI-based models, including **SVM** (Support Vector Machine), **RF** (Random Forest), **XGBoost** (Extreme Gradient Boosting), and deep learning (**DL**) approaches such as **CNN** (Convolutional Neural Network), contribute to robust tumor classification and prognosis. Explainable AI (**XAI**) techniques are increasingly being applied to enhance the interpretability and transparency of AI-driven diagnostic models, ensuring clinical trust and regulatory compliance. Additionally, advanced imaging techniques like **VIBE** (Volume Interpolated Breath-hold Examination) improve visualization. Attention-based methods like **CBAM** (Convolutional Block Attention Module) and multi-scale feature extraction via **ASPP** (Atrous Spatial Pyramid Pooling) further enhance segmentation accuracy., **AUC** (Area Under the Curve), and **CI** (Confidence Interval) provide quantitative insights into model performance. Odds-based assessments such as **OR** (Odds Ratio) are also used for statistical validation. Emerging techniques using **GAN** (Generative Adversarial Network) aid in data augmentation and stain normalization, while transformer-based models like **ViT** (Vision Transformer) show promise in histopathological and imaging analysis.

II. CAUSES OF LIVER TUMOURS

The etiology of liver tumours is diverse, and involves a combination of genetic, environmental, as well as lifestyle factors. Chronic infection with hepatitis B and C viruses comes up as the leading cause of liver cancer globally. The chronic infection that comes from hepatitis B and C viruses is one of the leading causes of liver cancer worldwide, contributing to the development of HCC.

Other significant risk factors include chronic alcohol consumption, which can lead to cirrhosis and subsequently liver cancer, as well as NAFLD, which is increasingly recognized as a major cause due to rising obesity rates. Other than that, exposure to aflatoxins is also a prominent cause of Liver Tumours [4], also the toxic compounds produced by certain fungi in food, and genetic conditions

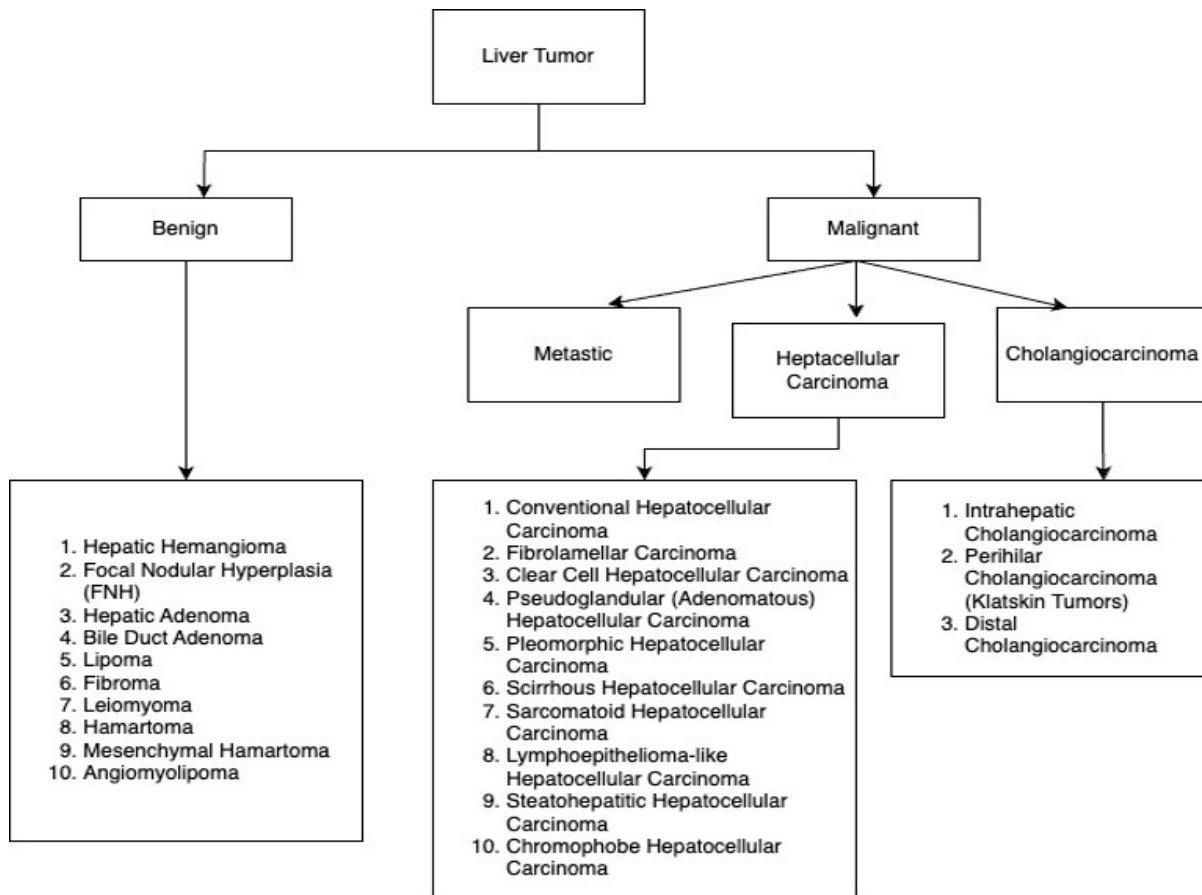


FIGURE 1. Liver tumor classification chart.

like hemochromatosis play crucial roles in liver tumour development [5], [6]. There have been a surge in cases where the prolonged use of OCPs has also been associated with an increased risk of benign liver tumours, such as hepatic adenomas, which have the potential to become malignant over time [7].

Certain inherited metabolic disorders, such as Wilson's disease and alpha-1 antitrypsin deficiency, can increase the risk of liver tumours. A familial history of liver cancer can also indicate a genetic predisposition [8].

Diabetes is also considered a contributing factor to malignant liver tumours. Both type 2 diabetes and insulin resistance have been linked to an increased risk of liver cancer, possibly due to their association with NAFLD and metabolic syndrome [9]. Obesity is a significant risk factor for NAFLD, which can progress to NASH and increase the risk of developing liver cancer. Cirrhosis, caused by conditions such as autoimmune hepatitis, primary biliary cholangitis, or primary sclerosing cholangitis, can increase the risk of liver cancer [10].

Cirrhosis is a condition marked by scarring of the liver tissue due to long-term damage, which can significantly elevate the risk of malignant transformation. Smoking has been associated with an increased risk of liver cancer, as the carcinogens in tobacco can contribute to liver damage and

cancer development. Consumption of food contaminated with aflatoxins, produced by *Aspergillus* species fungi, is a well-known risk factor for liver cancer, particularly in certain regions where food storage conditions promote fungal growth [6]. Long-term exposure to certain chemicals, such as vinyl chloride and thorium dioxide (Thorotrast), which were used in industrial applications and medical procedures respectively, can increase the risk of developing liver cancer [11]. The use of anabolic steroids, often by athletes for performance enhancement, has been linked to liver tumours, including hepatic adenomas and hepatocellular carcinoma. Chronic infection with liver flukes, such as *Opisthorchis viverrini* and *Clonorchis sinensis*, is a risk factor for cholangiocarcinoma, a type of liver cancer that affects the bile ducts [12].

III. LIVER TUMOUR CLASSIFICATION

Liver tumours are primarily classified into benign and malignant categories as shown in Figure 1. Each category includes various types based on their site of origin and prevalence.

A. BENIGN LIVER TUMOURS

Benign liver tumours are non-cancerous growths that generally do not spread to other parts of the body. Despite being

non-malignant, they can still cause significant health issues if they grow large or are located near critical structures [13], [14].

- **Hepatic Haemangioma:** The most common benign liver tumour, often found incidentally during imaging studies. These are composed of clusters of blood vessels and typically do not cause symptoms unless they are of a significant size [15].
- **Focal Nodular Hyperplasia (FNH):** It is considered as the second most common benign liver tumour type, and it is usually asymptomatic and discovered incidentally. FNH consists of a mixture of hepatocytes, bile duct cells, and connective tissue [16].
- **Hepatic Adenoma:** It is comparatively less common but significant due to its potential to become malignant or cause bleeding. It is often associated with the use of oral contraceptives and anabolic steroids [15].
- **Bile Duct Adenoma:** It is considered as one of the rarer types of benign tumour, and it originates from the bile duct epithelium. It is usually small and asymptomatic [16].
- **Lipoma:** Is a significantly rare benign tumour composed of fatty tissue. It is typically asymptomatic and discovered incidentally [15].
- **Fibroma:** A benign tumour of fibrous connective tissue. It is extremely rare in the liver [15].
- **Leiomyoma:** A rare benign tumour of smooth muscle origin. These are very uncommon in the liver [15].
- **Hamartoma:** A benign, tumor-like malformation consisting of an abnormal mixture of cells and tissues that are native to the liver. It is considered one of the rarer types of benign tumours, typically originating from the bile duct epithelium [15].
- **Mesenchymal Hamartoma:** A rare benign liver tumour that usually occurs in infants and young children. It is composed of mesenchymal tissue [17].
- **Angiomyolipoma:** A rare benign tumour composed of blood vessels, smooth muscle, and fat. More commonly seen in the kidneys but can occur in the liver [15].

B. MALIGNANT LIVER TUMOURS

Malignant liver tumours are cancerous and can spread to other parts of the body. They are further divided into primary liver cancers (originating in the liver) and secondary liver cancers (metastatic tumours from other organs) [18].

- **HCC:** The most common primary liver cancer, accounting for about 75% of all liver cancers. It typically arises in the context of chronic liver disease, particularly cirrhosis due to hepatitis B, hepatitis C, or alcohol use. There are various subtypes of HCC [19]:

- **Conventional HCC:** This is the most prevalent form, often associated with cirrhosis and chronic liver disease. It typically presents with a heterogeneous appearance and is characterized by the proliferation of hepatocytes and loss of normal liver architecture [20].

- **Fibrolamellar Carcinoma:** A rare, well-differentiated subtype of HCC that tends to occur in younger individuals without any underlying liver disease. It is often diagnosed at an early stage and tends to have a better prognosis compared to other forms of HCC. It is characterized by large, well-formed fibrous bands and relatively normal liver architecture [21].
- **Clear Cell Hepatocellular Carcinoma:** This subtype is defined by hepatocytes that appear clear under the microscope due to the accumulation of glycogen and fat. These clear cells give the tumor a distinctive appearance and are associated with more aggressive disease progression.
- **Pseudo glandular (Adenomatous) Hepatocellular Carcinoma:** This variant features structures that resemble glands, though they are not true glands. These tumours often demonstrate a disorganized growth pattern that makes them harder to classify as typical HCC [14].
- **Pleomorphic Hepatocellular:** This subtype contains highly varied and abnormal cell shapes, often reflecting more aggressive and invasive behavior. The presence of pleomorphic cells is an indication of rapid tumor growth and poor prognosis [22].
- **Scirrhouss Hepatocellular Carcinoma:** Characterized by abundant fibrous tissue within the tumor, scirrhouss HCC tends to be harder and more densely fibrotic. This subtype can lead to a more restrictive and stiffer liver, complicating the overall clinical picture [22].
- **Sarcomatous Hepatocellular Carcinoma:** This subtype contains both carcinoma (epithelial) and sarcoma-like (mesenchymal) elements. The presence of sarcomatous features often implies a more aggressive tumor, with poor response to standard therapies [22].
- **Lymphoepithelioma-like Hepatocellular Carcinoma:** This rare subtype of HCC resembles lymphoepitheliomas, a type of tumor seen in the nasopharynx. It typically shows an admixture of hepatocellular carcinoma cells and lymphocytes, often indicating an immune-mediated component to its development [22].
- **Steatohepatitis Hepatocellular Carcinoma:** Associated with NASH, this subtype of HCC is commonly linked to metabolic conditions like obesity, diabetes, and NAFLD. The presence of fatty liver changes, along with inflammation, contributes to the increased risk of developing HCC [18], [22].
- **Chromophobe Hepatocellular Carcinoma:** This subtype is characterized by cells that stain lightly and appear pale due to the lack of specific cellular structures. The presence of chromophobe cells can

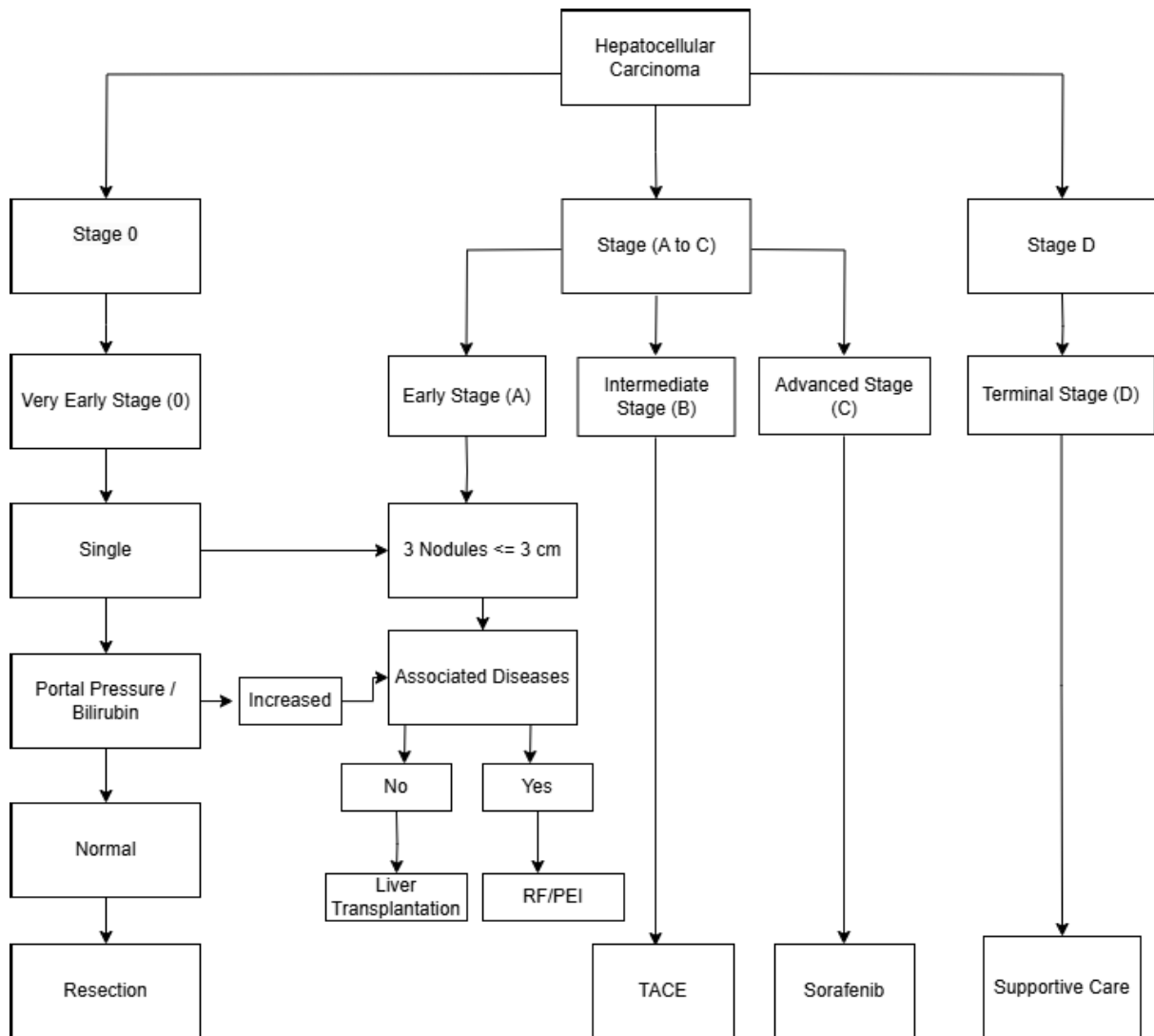


FIGURE 2. Staging of Hepatocellular Carcinoma.

indicate a distinct genetic profile and may influence prognosis and treatment options [22].

Cholangiocarcinoma: Cholangiocarcinoma is a type of cancer that originates in the bile ducts, which are responsible for carrying bile from the liver to the small intestine. Cholangiocarcinomas are classified based on their location within the bile duct system [18]:

- **Intrahepatic Cholangiocarcinoma:** Arising within the bile ducts inside the liver, this is the second most common primary liver cancer after HCC. It often presents with obstructive jaundice and is associated with conditions like primary sclerosing cholangitis, liver cirrhosis, or hepatitis C. The prognosis for intrahepatic cholangiocarcinoma is generally poor, as it is often diagnosed at a later stage [23].
- **Perihilar Cholangiocarcinoma (Klatskin tumours):** This form of cholangiocarcinoma develops at the junction where the right and left hepatic ducts merge,

forming the common hepatic duct. It is often challenging to diagnose early due to its location and the nonspecific symptoms it causes. Klatskin tumours are frequently diagnosed in the advanced stages and are typically treated with surgery, though recurrence is common [24].

• **Distal Cholangiocarcinoma:** These tumours arise in the bile ducts outside the liver, closer to the junction with the small intestine. They are more likely to cause obstructive jaundice and can present with symptoms related to biliary obstruction, such as pain, fever, and weight loss. Surgical resection is often the treatment of choice, but prognosis is typically poor once the disease has spread [25].

Metastatic Liver Cancer: It is a Secondary liver cancer that originates from other organs and then further spreads to the liver. The cancer usually spreads from colon, breast, lung, pancreas and stomach to the liver due to liver's rich blood supply and filtration [26].

IV. STAGING OF LIVER CANCER

The staging of cancer in livers, specifically HCC, it is very important for figuring out the exact treatment that has to be given to a patient for the right outcomes, Staging is done on many factors, on the basis of the size of the tumours, the extent of the spread within the liver. There are various staging systems used globally the Barcelona Clinic Liver Cancer(BCLC) staging system is the most widely used staging tumours, it incorporates tumour characteristics, liver function, and patient performance status [28].

A. BCLC STAGING SYSTEM

The BCLC staging system divides liver cancer into several stages, each of these stages are associated with specific treatment recommendations:

Stage 0 (Very Early Stage)

- **Characteristics:** A single tumour less than 2 cm in size, without vascular invasion or spread to lymph nodes or distant sites.
- **Treatment:** Surgical resection is typically recommended if the patient's liver function is preserved and portal pressure and bilirubin levels are normal.

Stage A (Early Stage)

- **Characteristics:** Up to three nodules, each less than or equal to 3 cm in size.
- **Treatment:** Potential curative treatments include surgical resection, liver transplantation, or RFA if the patient does not have associated diseases and portal pressure is not increased.

Stage B (Intermediate Stage)

- **Characteristics:** Multiple tumours that do not fit the criteria for stage A but have not spread beyond the liver.
- **Treatment:** TACE is the standard treatment, which involves injecting chemotherapy drugs directly into the liver's blood vessels to block the blood supply to the tumour.

Stage C (Advanced Stage)

- **Characteristics:** Tumours with vascular invasion or extrahepatic spread (metastasis).
- **Treatment:** Systemic therapies such as sorafenib, a targeted therapy that inhibits tumour growth and angiogenesis, are commonly used. Other systemic treatments may include newer targeted agents or immunotherapies.

Stage D (Terminal Stage)

- **Characteristics:** Patients with severe liver dysfunction (Child-Pugh C) or very poor performance status.
- **Treatment:** Focuses on palliative care to manage symptoms and improve quality of life. Supportive treatments may include pain management, nutritional support, and addressing other complications.

B. CHILD-PUGH CLASSIFICATION

The Child-Pugh classification system is frequently used in conjunction with tumour staging to evaluate liver function. It assesses five clinical parameters: bilirubin, serum albumin, prothrombin time, ascites, and hepatic encephalopathy.

Patients are divided into three groups based on these parameters (A, B, and C), with class A representing the best liver function and class C indicating the lowest [29].

C. OTHER STAGING SYSTEMS

Other staging methods include the TNM system, which stages cancer according to the size and number of primary tumours (T), the involvement of regional lymph nodes (N), and the existence of distant metastasis (M). The Okuda staging method and the Cancer of the Liver Italian Program (CLIP) score are both used to predict outcomes, both of which incorporate a variety of clinical and laboratory markers [30].

V. TREATMENT MODALITIES FOR LIVER TUMOURS

The kind, stage, and general condition of the patient all have a major impact on the therapy of liver tumours. The breadth of therapeutic techniques includes supportive care, systemic treatments, and surgical procedures as well as locoregional therapies. The main therapy options are outlined below, encompassing both traditional first therapies and modern approaches [31].

A. INITIAL TREATMENTS FOR LIVER TUMOURS

Initially, the Liver Tumour treatments were limited to surgical resection and palliative care. Surgical resection involved the removal of the tumour along with a margin of healthy tissue. This was considered the best curative option for localized tumours, particularly for patients with preserved liver function. However, many patients were not candidates for surgery due to the extent of their disease or poor liver function. Palliative care focused on alleviating symptoms and improving quality of life, but it did not address the tumour itself.

B. CURRENT TREATMENT OPTIONS

1) SURGICAL TREATMENTS

- **Liver Resection:** This involves the surgical removal of the tumour along with a portion of the surrounding healthy liver tissue. It is the treatment of choice for patients with early-stage liver cancer and good liver function. Advances in surgical techniques and perioperative care have improved the outcomes of liver resection [32].

- **Liver Transplantation:** This involves replacing the diseased liver with a healthy donor liver. It is particularly beneficial for patients with small, early-stage tumours (usually within the Milan criteria) who also have underlying cirrhosis. Transplantation offers a potential cure by removing both the tumour and the diseased liver tissue [31].

2) LOCOREGIONAL THERAPIES

- **Radiofrequency Ablation (RFA):** High frequency electrical currents in this form of this minimally invasive procedure generates heat and destroy cancer cells. For

- small tumours (usually less than 3 cm) it is well indicated when the patient is not suitable for surgery [26].
- **TACE:** In TACE chemotherapy drugs are delivered directly to the tumour in the liver via the hepatic artery, with particles injected to block the blood supply to the tumour. This method is typically used for tumours that are not surgically or ablated amenable for intermediate stage tumours [33].
 - **TARE:** TARE delivers radioactive particles to the tumour by way of the hepatic artery. It shrinks the tumour with the help of radiation, while damaging the healthy surrounding tissue less [34].
 - **Percutaneous Ethanol Injection (PEI):** That means injecting ethanol directly through the tumour to kill the cells. However, PEI is not widely used today because newer, more efficient means of ablation such as RFA are available [35].

3) SYSTEMIC THERAPIES

- **Targeted Therapies:** Sorafenib, Lenvatinib and regorafenib [40] are drugs targeting specific pathways that lead to tumour growth and angiogenesis. The first systemic therapy approved for advanced HCC, Sorafenib, has been shown to improve survival [36].
- **Immunotherapy:** However, advanced liver cancer is treated by checkpoint inhibitors like nivolumab and pembrolizumab. These drugs increase the system's ability to recognize and destroy cancer cells [36].
- **Chemotherapy:** Liver cancer is extremely hard to beat, thanks to the liver's power of detoxing drugs, thus in liver cancer, systemic chemotherapy has limited effectiveness. However, it may be used under certain circumstances [37].

4) SUPPORTIVE AND PALLIATIVE CARE

- **Symptom Management:** Supportive care focuses on alleviating symptoms such as pain, jaundice, and ascites to improve the quality of life for patients with advanced liver cancer [38].
- **Nutritional Support:** Ensuring adequate nutrition is crucial for patients with liver cancer, particularly those with cirrhosis, to maintain strength and overall health [39].

Emerging Treatments: Emerging treatments for liver cancer are very important in addressing the challenges that are associated with this aggressive disease. One of the most promising recent approach is the combination of Stereotactic Body Radiotherapy(SBRT) and immunotherapy [41]. In SBRT precise, high doses of radiation to the tumour are delivered, while sparing surrounding healthy tissue, which makes it an effective option for targeting liver tumours. Whereas Immunotherapy, on the other hand, utilizes the body's immune system to identify and destroy cancer cells. Combining these two modalities leverages their synergistic effects, which potentially enhances the overall treatment

efficacy for patients with HCC. The trial had been done on 100 patients which had nonmetastatic, unresectable HCC, out of the 100 patients, 70 patients underwent SBRT alone, which 30 patients received the combination of SBRT with immunotherapy. The trial revealed that the group which received the SBRT treatment in combination with Immunotherapy had a considerably better overall survival rates, with 1- year and 3-year OS rates of 92.0% and 63.9%, respectively, in comparison of 74.0% in 1-year OS and 43.3% in 3-year OS [41].

Apart from the high survival rates the SBRT-IO therapy also showed better results in terms of TOP and the ORR. The study mentioned that the patients who were treated with SBRT-IO has a higher ORR of 88%, overall response rate. The study discovered that the SBRT-IO group had a higher ORR of 88%, with 56% obtaining a full response and 22% getting a partial response. While the patients who received only the SBRT treatment developed grade 3 or higher immune-related side effects, such as hepatitis and dermatitis, these were treatable and did not have a major influence on the therapy's overall benefits [41].

The SBRT and immunotherapy combination gave benchmark results on the trials and outperformed the SBRT alone, which shows that SBRT along with immunotherapy has the potential of becoming the new standard treatment, as this method boosts the anti-tumour immune response and also precisely targets the tumour with radiation, potentially enhances the life survival chances of patient as well as improves the quality of patients life.

VI. AI IN LIVER TUMOUR AND LIVER CANCER DIAGNOSIS

Artificial Intelligence (AI) has made significant contributions to the diagnosis and management of liver tumours and liver cancer, transforming traditional diagnostic workflows through its ability to analyze complex imaging and histopathological data. Recent deep learning models have demonstrated diagnostic accuracy that approaches or even exceeds expert clinician performance, while also reducing analysis time and standardizing interpretation across institutions [47], [102]. For example, in a controlled reader study by Kiani et al. [47], a DenseNet-based classifier was evaluated against 11 practicing pathologists in classifying HCC versus CC on whole-slide histology images. The study found that when the AI prediction was correct, the odds of a correct diagnosis by a pathologist increased by a factor of 4.289 (95% CI: 2.360—7.794), while incorrect AI predictions reduced the odds to 0.253 (95% CI: 0.126—0.507). Similarly, Wang et al. [102] reported that their AI model outperformed expert radiologists in classifying liver lesions on MRI, while also offering interpretability through lesion heatmaps and enhancement feature tracking.

These innovations span diverse applications—from enhancing radiological interpretation to automating the analysis of histopathological slides—and are contributing to improvements in diagnostic accuracy, early detection, personalized treatment planning, and longitudinal disease

TABLE 1. Preprocessing techniques for histopathological analysis of liver tissues.

Preprocessing Technique	Purpose	Advantages	Challenges/Limitations
Stain Normalization [45]	Standardize color variations in histopathological slides	Ensures consistency across datasets and improves model generalizability	Computationally expensive; sensitive to staining protocols
Histogram Equalization [46]	Enhance contrast in images	Highlights features, making them more distinguishable for models	May amplify noise in certain regions
Patch Extraction [48]	Divide large WSIs into smaller patches for processing	Enables handling of high-resolution images; reduces computational cost	Requires careful selection of patch size to maintain contextual information
Data Augmentation [49]	Increase dataset diversity artificially (e.g., rotations, flips, color variations)	Reduces overfitting; improves generalization on unseen data	May introduce unrealistic data artifacts if not done carefully
Edge Detection [52]	Highlight boundaries of nuclei and structures in images	Enhances segmentation accuracy by focusing on critical features	Sensitive to noise and may misinterpret overlapping nuclei
Color Normalization [47]	Match the color distribution across different histological images	Minimizes batch effects and dataset inconsistencies	Requires representative reference images
Anisotropic Diffusion [51]	Reduce noise while preserving edges	Retains important features; useful for segmentation tasks	Computationally intensive; sensitive to parameter selection

monitoring [42]. A summary of common pre-processing techniques used in histopathological analysis of liver tissues, including their objectives, benefits, and limitations, is presented in Table 1.

Deep learning-based algorithms, particularly CNNs and more recently Transformer-based models, have advanced liver lesion classification and segmentation accuracy in both CT and MRI modalities. Beyond imaging, AI systems are increasingly being applied to histopathological data for identifying early cellular changes indicative of malignancy, grading tumors, and predicting patient-specific outcomes [43].

In this review, we categorize recent AI-driven advancements in liver cancer diagnosis into three primary domains: (1) AI applications in histopathological analysis for cancer detection and grading; (2) AI-based segmentation and classification of liver and tumor regions from radiological imaging; and (3) emerging integrative approaches, including prognosis prediction, radiomics-based risk stratification, and multimodal fusion of imaging, clinical, and genetic data.

VII. AI APPLICATIONS IN THE HISTOPATHOLOGICAL ANALYSIS OF LIVER TISSUES

Histopathology remains crucial for diagnosing and planning the treatment of HCC, yet manual analysis of histological slides is time-consuming and prone to variability. By leveraging AI-driven systems, these slides can be interpreted more consistently and efficiently, thereby reducing diagnostic errors [44]. The following sections examine six key roles that AI plays in the histopathological analysis of liver cancer: (1) classification between normal and malignant tissues, (2) tumour classification and staging, (3) nuclei segmentation, (4) liver cancer segmentation in whole slide images (WSI), (5) binary classification of liver cancer and mutation prediction, and (6) the use of liver histopathology datasets to train and validate these models.

A. CLASSIFICATION BETWEEN NORMAL AND MALIGNANT TISSUES

One of the primary tasks in liver cancer diagnosis is distinguishing between healthy and cancerous tissue. This process is crucial for identifying the presence of tumours

and initiating the appropriate treatment. AI models, trained on large datasets of histological images, can be used to automatically classify tissue samples as either normal or malignant, helping pathologists make faster and more accurate diagnoses. By reducing subjectivity and human error, AI can improve the overall reliability of liver cancer detection [44].

In histopathology image analysis, weakly supervised learning refers to approaches that do not rely on dense or pixel-level labels for every patch in a slide. Instead, only coarse slide-level (e.g., ‘this slide is HCC vs. iCCA’) or region-level (‘this region is tumor vs. non-tumor’) annotations are available. Such methods typically involve two phases: (1) training a feature extractor or a classification network using the limited labels, often focusing on distinguishing tumor from normal tissue, and (2) applying unsupervised or clustering-based techniques on the learned features to differentiate subtypes. This strategy drastically reduces the annotation burden for pathologists, who otherwise must provide highly detailed labels at the patch or cellular scale. By exploiting CNN-based representations—sometimes in conjunction with clustering or multiple-instance learning—weak supervision can yield high diagnostic accuracy even in large-scale WSI analyses, as demonstrated by Beaufrère et al. [45] and others.

Beaufrère et al. [45] implemented a patch-based, weakly supervised pipeline to classify primary liver cancers (PLCs) from routine biopsy slides using a ResNet18 architecture. Specifically, they digitized 166 PLC biopsies (split into training [90 samples], internal validation [29], and external validation [47]), each scanned at high magnification. From each whole-slide image (WSI), they extracted 256×256 pixel patches—focusing on tumor areas via manual tumor/non-tumor annotation—ultimately generating 1,863,132 training patches and 23,804 validation patches. The network (pre-trained on ImageNet) was fine-tuned on these patches under weak supervision, relying only on tumor vs. non-tumor labels rather than detailed subtype annotations. After feature extraction from the last convolutional layer of ResNet18, a Gaussian mixture model clustered patches into HCC—like or intrahepatic cholangiocarcinoma (iCCA)—like groups. Despite combined HCC—cholangiocarcinoma

(cHCC-CCA) not forming its own distinct cluster, the approach achieved 97% accuracy for HCC and 83% accuracy for iCCA on the external validation set—showcasing that minimal annotation (weak supervision) can effectively classify liver cancers from limited biopsy material.

An advanced approach employing ResNet-based architectures for liver cancer histopathology image classification was presented by Sun et al. [46]. The authors applied histogram equalization and a stain normalization method based on a Generative Adversarial Network (GAN)—a deep learning framework consisting of a generator and discriminator trained in opposition to produce highly realistic synthetic data. The stain GAN was used to standardize color variations across different pathology slides, ensuring consistency in image appearance and reducing batch effects. The model was trained on the TCGA-LIHC dataset, which included 462 tissue slide images—comprising 79 normal liver histopathology images and 383 HCC images. Classification performance was excellent on the validation dataset, with recall = 0.99 and precision = 0.99. This study highlighted that applying global labels in combination with advanced normalization techniques can significantly improve liver cancer classification performance in histopathological image analysis.

Kiani et al. [47], developed a diagnostic support tool that integrates a DL based assistant into the pathology workflow to differentiate between HCC and CC on WSI of H&E-stained tissue. The AI model underpinning the assistant was built using a CNN with a DenseNet architecture. DenseNet was chosen for its dense connectivity, which facilitates improved feature propagation and mitigates the vanishing gradient problem—key advantages for handling the complex visual patterns present in histopathological images. The model was trained on 25,000 non-overlapping image patches of size 512×512 pixels, extracted from 70 WSIs (balanced between 35 HCC and 35 CC cases) derived from formalin-fixed, paraffin-embedded(FFPE) primary tumor resections. In addition to producing diagnostic probabilities for HCC and CC, the model generates class activation maps(CAMs) that highlight the image regions most influential in its decision-making. In a carefully designed crossover study involving 11 pathologists with varying levels of expertise, the tool's impact was evaluated. When the AI model's prediction was correct, the odds of a pathologist making a correct diagnosis increased by a factor of 4.289 (95% CI: 2.360—7.794). Conversely, when the model's prediction was incorrect, the odds dropped significantly (OR = 0.253, 95% CI: 0.126—0.507). These results demonstrate that while the DenseNet-based assistant can substantially enhance diagnostic performance, particularly in challenging cases, it also poses risks of automation bias if its outputs are erroneous.

Lin et al. [48] conducted a systematic study to quantify how the size of the annotated training dataset affects the classification accuracy in HCC histopathology image analysis. They employed the GoogLeNet (Inception-V1) architecture, which is renowned for its inception modules

that combine multiple convolutional kernels of varying sizes, to capture diverse spatial features from image patches extracted from 29 whole-slide images (WSIs). In their experimental setup, each WSI was cropped into patches of 448×448 pixels, which were subsequently resized to 224×224 pixels to meet the input requirements of GoogLeNet. This resizing not only standardized the input but also preserved critical morphological details. The model achieved an overall accuracy of 91.37%, with specificity and sensitivity recorded at 90.57% and 92.16%, respectively. To further understand the data dependency of the model's performance, Lin et al. developed an inverse power law function-based estimation model. This model fits the observed learning curve—which depicts the classification accuracy as a function of the training dataset size—using a function of the form: $y = 100 + b_1 \cdot x^{b_2}$, where y represents the classification accuracy, x is the number of training images, and b_1 and b_2 are parameters corresponding to the learning rate and decay rate, respectively. Parameter estimation was performed using weighted nonlinear least squares optimization to accurately capture the asymptotic behavior of the model as it approaches the maximum achievable accuracy. Their analysis demonstrated that classification accuracy improves significantly with increased training data, and the fitted curve provided a practical method to predict the minimum number of annotated images required to reach a desired diagnostic performance threshold. This approach not only highlights the importance of dataset size in deep learning but also provides valuable guidance for resource allocation in clinical annotation efforts.

B. CLASSIFICATION AND STAGING OF TUMOURS

A Machine learning model can do more than just detect whether there is cancer present, it can tell what stage the tumour is and that is a critical piece of information when looking at treatment plans. The size, spread and aggressiveness of the tumour is shown by the staging; an AI based systems can help streamline this process by using histopathological features to classify tumour types and stage. These types of systems present a more detailed understanding of tumour progression and are increasingly used to help design personalized treatment strategies.

Chen et al. [49] developed a deep learning approach that leverages the Inception V3 architecture to classify liver tumours and predict histopathological grades directly from H&E-stained WSIs. In their study, a dataset of 491 WSIs was used—comprising 89 normal liver tissues and 402 WSIs of HCC. Among the HCC cases, 383 WSIs contained detailed annotations for histopathological grading, which allowed the tumours to be stratified into well-differentiated (G1), moderately differentiated (G2), and poorly differentiated (G3/G4) groups. The Inception V3 model, pre-trained on the ImageNet dataset, was fine-tuned on image patches extracted from these WSIs. Its architecture is characterized by multiple inception modules that integrate convolutional filters of varying kernel sizes along with max-pooling layers,

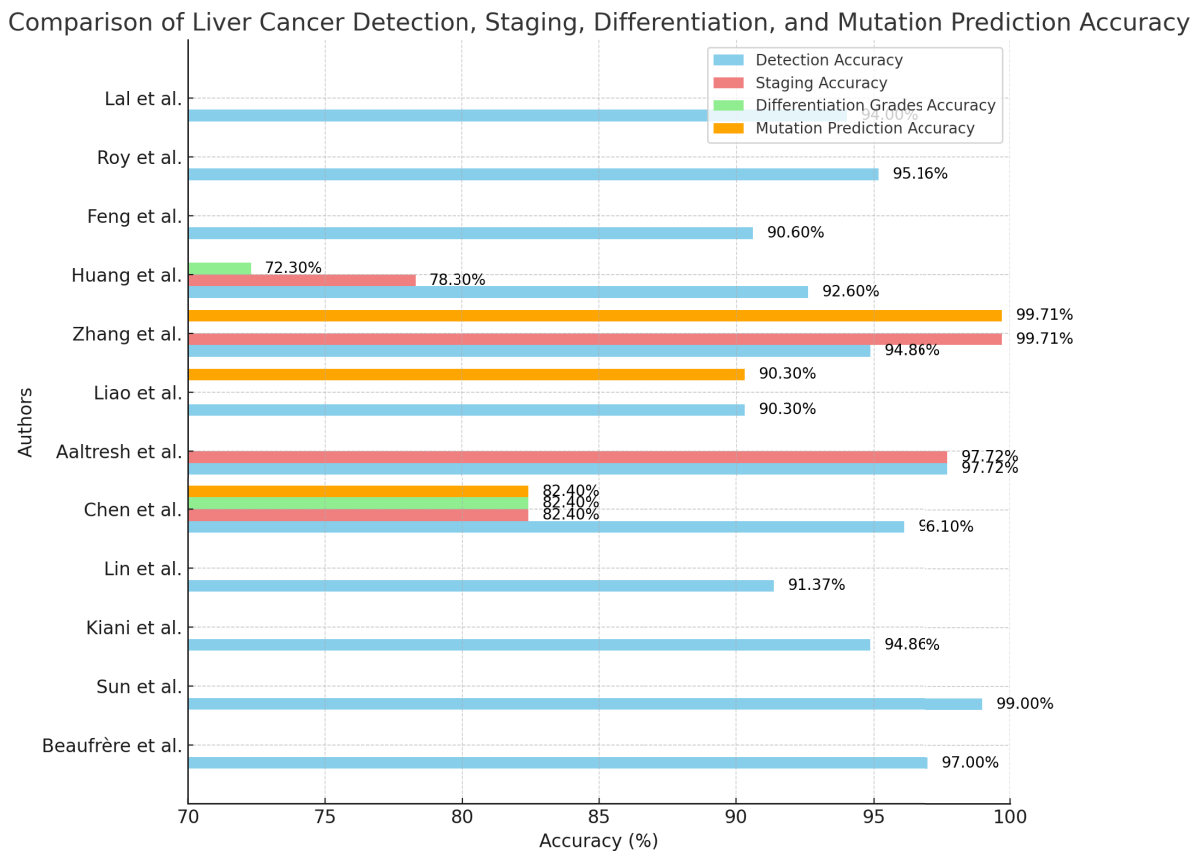


FIGURE 3. Comparison of liver cancer detection from histopathology, staging Differentiation and Mutation prediction accuracy across different literature.

which collectively facilitate the extraction of rich, multi-scale features. This design enables the network to capture subtle morphological cues critical for differentiating between normal and cancerous tissues and for assessing tumour grade. During training, extensive pre-processing—such as stain normalization and patch resizing (typically to 224×224 pixels to match the network’s input requirements)—was applied to ensure consistent input quality. The model achieved an impressive area under the ROC curve (AUC) of 0.961 in classifying benign versus malignant tissues, with a Matthews correlation coefficient (MCC) of 0.82, indicating robust discriminative power. For tumour grading, the model reached an MCC of 0.738, reflecting its ability to differentiate between the gradations of tumour differentiation.

Aatresh et al. [50] introduced LiverNet, a specialized deep learning architecture tailored for classifying liver histopathology images into multiple HCC subtypes. Their model adopts a convolutional pipeline with Convolutional Block Attention Modules (CBAM) and Atrous Spatial Pyramid Pooling (ASPP) blocks to capture both local cellular features and multi-scale contextual cues from H&E-stained images. Concretely, LiverNet processes images in an encoder–decoder-like fashion, where the encoder incorporates residual connections, CBAM modules for channel/spatial attention, and ASPP layers at various depths to extract robust

multi-scale representations of nuclei morphology and tissue architecture. In their experiments, Aatresh et al. evaluated the model on both the KMC dataset (257 total liver biopsy slides across four classes) and the TCGA-Liver dataset (141 slides). For each dataset, fivefold cross-validation was performed using patch extraction (e.g., 1000×1000 or 1024×1024 patches). After training, LiverNet achieved 90.93% accuracy on the KMC dataset and 97.72% accuracy on the TCGA-Liver dataset, outperforming several state-of-the-art networks (e.g., DenseNet, InceptionResNetV2). Notably, their architecture required only 0.57 million parameters and 1.19 million Floating Point Operations(FLOPs), reflecting a highly efficient design. By integrating bilinear upsampling instead of transposed convolutions and leveraging depthwise separable convolutions within ASPP, LiverNet demonstrated that accurate multi-class HCC subtype classification can be attained with minimal computational overhead, making it a robust solution for real-world histopathological diagnosis.

C. NUCLEI SEGMENTATION

Nuclei segmentation refers to identifying and outlining cell nuclei in histopathological tissue samples. It is essential for tumour grading, as nuclear size, shape, and spatial distribution are key indicators of malignancy.

Conventional approaches typically involve tedious and sometimes error-prone manual analysis of numerous images to quantify morphological features. AI-based segmentation tools, by contrast, can partially or fully automate this process, achieving higher accuracy in significantly less time. Such automated systems assist pathologists in evaluating tumour aggressiveness and guiding prognosis, ultimately improving patient care.

In order to address difficulties that arise from variability of shapes and touching nuclei in liver cancer histopathology image segmentation, Lal et al. [51], presented a new model called NucleiSegNet. The proposed architecture used a residual block as well as a tailored attention mechanism to improve the extraction of spatial features and the use of features. NucleiSegNet was tested for its performance on the KMC liver dataset and the Kumar dataset in which the latter outperforms the former through an enhancement on the F1 score and Jaccard Index (JI) which were increased by 3% on the KMC dataset and up to 1.2% on the Kumar dataset. The proposed model for medical segmentation outcompeted other segmentation models using only 13 million parameters, while maintaining efficiency and high accuracy levels.

To address the problem of nuclei segmentation in liver cancer histopathological images, Roy et al. [52] propose a multi-step, standard-deviation-based edge detection pipeline that explicitly tackles noise and staining inconsistencies. First, they employ a color normalization step as a preprocessing phase, which helps reduce inter-slide staining variability. Rather than using gradients, their core edge-detection strategy computes local standard deviations in an $s \times s$ neighborhood around each pixel. Because local standard deviation is highly correlated with the presence of edges—and is far less sensitive to small intensity fluctuations—this method mitigates many noise-related artifacts that plague traditional gradient-based edge detectors. After deriving an edge map, Roy et al. [52] convert the image to a binary mask using Otsu's thresholding, which automatically determines the optimum cutoff to separate foreground (nuclei) from background. They then apply an adaptive morphological filter to refine the segmentation. Unlike fixed-size structuring elements, this filter's kernel size is adjusted via a fuzzy function that measures how much local standard deviation differs from the global standard deviation. In regions with higher apparent noise, the structuring element expands slightly to remove cluttered artifacts (e.g., red blood cells or random speckles); in regions with lower noise, the filter contracts to preserve fine boundary details. By combining these steps—color normalization, local-std-based edge detection, Otsu thresholding, and an adaptive morphology pass—the authors achieve both high accuracy and low noise in the resulting segmentation. On the Kumar multi-organ dataset, the approach attains an F1 score of 0.9516, a Jaccard Index of 0.8291, and a PSNR(Peak Signal-to-Noise Ratio) of 19.174, with a CPU processing time of about 4.2 minute per image. These metrics indicate that Roy et al.'s method not only competes with but can sometimes outperform

deep-learning pipelines—such as DIST or MicroNet—while retaining a fully unsupervised workflow that does not rely on ground-truth masks for training.

Huang et al. [53] proposed a novel histopathological diagnostic framework for liver cancer that integrates Raman spectroscopic imaging with a deep learning pipeline based on a one-dimensional variant of the VGG-16 architecture. Their model adapts the classical VGG-16 structure—comprising 13 convolutional layers, 5 max-pooling layers, and 3 fully connected layers—to process sequential spectral data in the 500–2000 cm⁻¹ range. Prior to network input, Raman spectra are preprocessed through baseline subtraction and smoothing to mitigate fluorescence background and noise artifacts. The small 3×3 convolutional kernels in VGG-16 are noted to be effective for capturing subtle spectral fluctuations associated with biochemical differences between tumor and non-tumor tissues. While VGG-16 is relatively parameter-intensive compared to more recent architectures like EfficientNet or Vision Transformers (ViT), the authors selected it based on its established performance and architectural compatibility with their Raman spectral analysis pipeline. However, no empirical comparison with other deep learning architectures was performed in the study.

The model was evaluated on a curated dataset containing Raman spectra from both carcinoma and adjacent non-tumorous liver regions. It achieved a classification accuracy of 92.6%, with a sensitivity of 90.8% and specificity of 94.6% for identifying carcinoma tissue areas. Training employed randomized batching, learning rate optimization, and dropout regularization to minimize overfitting—an important consideration given the inherent heterogeneity of tumor samples. In addition to the binary classification task, Huang et al. also trained three separate CNN models to address more granular classification goals, including tumor staging and histological differentiation. These models achieved accuracies of 78.3% for tumor stage classification and 72.3% for grading tumor differentiation. The highest performance was observed in distinguishing between HCC and ICC, where the model achieved 82.4% accuracy. While these results demonstrate the feasibility of Raman-enhanced deep learning for liver cancer pathology, the study acknowledges ongoing challenges related to tumor heterogeneity and spectral variability. Future work will explore lighter-weight network architectures and further optimization of spectral preprocessing to improve model generalizability across diverse patient populations.

D. LIVER CANCER SEGMENTATION IN WSI

Digital WSI offer a broad survey view of the samples at high magnification making it a valuable asset especially in liver cancer diagnosis. However, because the size and nature of WSIs create challenges for automated segmentation, it is difficult to differentiate the tumours from the surrounding benign tissue. Due to variations in tissue structure, staining, and scale, effective segmentation of liver cancer in WSIs

demands stringent and stabilized algorithms. advances in machine learning, particularly through the deployment of advanced CNNs such as U-Net variants and hybrid models, significant progress has been achieved in segmenting liver tumours in whole slide images. Some of the current research findings have, therefore, focused on analysing the multi-scale architectures and using post-processing strategies that enhance segmentation precision in WSIs to enhance pathologists' identification of carcinogenic areas. In this section, we explore newly developed approaches and technologies of liver cancer segmentation on WSI with emphasis on multi-scale concept and deep learning architecture.

In focus on the segmentation of liver cancer areas in WSIs, Feng et al. [54], adopted multi-scale deep learning of 3D U-Net architecture. The model was tested on the data set of the MICCAI PAIP Challenge 2018 which comprised 50 training WSIs, 10 validation WSIs and 40 testing WSIs. It employed a seven-level Gaussian pyramid for multi-scale representation, and a voting strategy in order to improve the segmentation performance. The model obtained best F1 of 0.906 and Jaccard of 0.805 on the given challenge than the other Kirilova et al. [71] studied the State-of-The-Art methods. Also, the Harsdorf distance where U-Net was trained on was 4.793, which show that the segmentation of this model is better. This work showed that the multi-scale approach combined with partial colour normalisation and weighted overlap improves the quality of segmentation in images of liver histopathology.

E. BINARY CLASSIFICATION OF LIVER CANCER AND MUTATION PREDICTION

Right diagnosis of liver cancer and prognosis of genetic changes are critical for estimating the most appropriate lines of treatment. Recent progress in advanced deep learning architectures—particularly CNNs and Transformer-based models—has enabled the automation of tasks such as histopathological image analysis for liver cancer classification and mutation prediction. In this section, additionally, we also discuss models that deliver not only a diagnosis of liver cancer, but also predict tumour mutation burdens and specific gene mutations to suggest targeted therapies. These methods are potent as good diagnostic methods as opposed to the conventional methods and could provide much insight on the development of cancer.

Liao et al. [55] developed a deep learning framework to both diagnose HCC and predict gene mutation features from histopathological images. Liao et al. constructed a CNN based on deep residual learning to overcome the degradation issues common in very deep networks. The model operates on 256×256 pixel tiles extracted from H&E-WSIs from TCGA and TMA dots from West China Hospital (WCH). In the classification task, the CNN was trained to distinguish HCC from adjacent normal tissue, achieving an outstanding per-tile AUC of 0.97. For mutation prediction, they adapted the classification CNN by replacing the final softmax layer

with a sigmoid layer, allowing the network to output mutation probabilities for key genes. Notably, the model predicted mutations in seven genes with high performance, achieving AUCs of 0.903 for CTNNB1 and 0.773 for TP53. This dual-task framework, which leverages the robustness of residual learning and detailed local features captured in 256×256 tiles, provides an automatic diagnostic tool and a promising method for predicting mutational profiles in HCC, thereby supporting precision medicine initiatives in liver cancer treatment.

Zhang et al. [56] did not use a pre-defined off-the-shelf architecture (such as VGG or ResNet) for their TMB estimation; instead, they developed a custom CNN tailored specifically for liver histopathology analysis. Their model comprises several convolutional layers that extract hierarchical features from the input images, followed by pooling layers to progressively reduce spatial dimensions while preserving critical local information. A key innovation in their approach was the systematic optimization of the receptive field size. Through a series of experiments, they identified that a 48×48 -pixel receptive field was optimal for capturing the subtle morphological characteristics—such as nuclear atypia and cellular density variations—that are indicative of tumor mutation burden. This custom network culminates in fully connected layers that integrate the extracted features to yield a binary classification of TMB status (high versus low). The model achieved a notable accuracy of 94.86% and an AUC of 0.9488 on data from TCGA-LIHC, and demonstrated a mean classification error of only 0.2994% at the case level, outperforming traditional panel sequencing methods. Overall, this tailored CNN approach offers a rapid, cost-effective alternative to conventional sequencing methodologies for TMB prognostication in liver cancer patients.

Chen et al. [49], investigated the feasibility of applying deep learning algorithms for predicting mutations in critical genes—specifically CTNNB1, FMN2, TP53, and ZFX4—from H&E-stained histopathological images of liver cancer. They leveraged the Inception V3 network, pre-trained on ImageNet, and fine-tuned it using a large dataset of liver tissue tiles extracted at $20\times$ magnification. Their model, implemented via the EASY DL platform and incorporating techniques from residual learning, achieved a benign-versus-malignant classification accuracy of 96.0% and histopathological grade classification accuracy of 89.6%. For mutation prediction, the network was modified by replacing the softmax layer with a sigmoid activation to output mutation probabilities. The model demonstrated robust performance with external AUCs ranging from 0.71 to 0.89, achieving particularly high predictive accuracy for CTNNB1 (AUC up to 0.903) and TP53 (AUC up to 0.773). These mutations are clinically significant, as they help predict patient outcomes with targeted therapies, such as TTK inhibitors used in HCC management. This work exemplifies how a tailored deep learning framework can decode the genetic structure of

TABLE 2. Datasets of Histopathological Slices (and Spectral Data).

Dataset	Cancer Subtype	Stain	Dimension	Image Format	Task	Annotation Types	Description
TCGA-LIHC	HCC	H&E	Varying	SVS	Classification	Image-level	<ul style="list-style-type: none"> Class Distribution: Commonly cited as 462 WSIs total (79 normal, 383 HCC). Some references mention 377 vs. 365 cases, reflecting slightly different curation. Lacks detailed pixel-level annotations for segmentation. Includes clinical, biological, survival, and pathological data (e.g., gene mutations). Dataset Splits: No official split; researchers often use 80% train / 20% test or other schemes. External Validation: Multi-center origin (TCGA). Some studies validate on independent cohorts (e.g., West China Hospital).
PAIP	HCC	H&E	Varying	SVS	Segmentation	Pixel-level	<ul style="list-style-type: none"> 100 WSIs (50 train, 40 test, 10 val). Ground-truth pixel masks for tumor areas. Single-center (Seoul Nat. Univ. Hosp.). External Validation: Not provided in challenge.
KMC	HCC	H&E	1920 × 1440	—	Classification, Segmentation	—	<ul style="list-style-type: none"> 257 WSIs, 4 sub-types: 70, 80, 83, 24. 80 WSIs with annotated nuclei. Class Distribution (patch-based): e.g. 3005 patches across normal / low- / medium- / high-grade. Dataset Splits: Not standardized; often 70–80% train, 20–30% test. External Validation: Typically validated against TCGA or other datasets.
GDC-Portal HCC data	HCC	H&E	Varying	SVS	Classification	Image-level	<ul style="list-style-type: none"> 491 WSIs: 402 HCC, 89 normal. Histopath. grade missing for 19 HCC WSIs. 387 HCC WSIs have mutation info. Dataset Splits: Often 80%/20%. External Validation: Multi-center (TCGA); some works add hospital cohorts.
Kumar Dataset	Multi-Organ	H&E	1000 × 1000	SVS	Nuclei Segmentation	Image-level	<ul style="list-style-type: none"> 30 H&E-stained images from 7 organs; 6 from liver. Typically 16 images train, 14 test. External Validation: None; single benchmark set. Variation in histology across organs.
Nature Raman Spectroscopy	Raman	—	—	Varying	Excel/CSV	Classification, Analysis	Spectrum-level <ul style="list-style-type: none"> 120 patient pairs (HCC vs. normal), 6000 spectra each class. Dataset Splits: No official ratio stated; authors used internal partition. External Validation: None reported; single-center data. Focuses on spectral analysis of liver tissues (not image-based).

tumours directly from histopathological images, supporting personalized treatment strategies in HCC.

F. LIVER HISTOPATHOLOGY DATASETS

The availability of the discussed datasets in the public domain is critical to the progress of AI based histopathological analysis. These datasets in Table 2. describe raw low-level patterns information and are used to train, test and validate models for making new algorithms more accurate and generalizable. The labelled histopathological images of the liver tissues are benchmarked in the datasets to encourage proper application and validation of AI models. Through such resources, it is possible for the AI community to add on to prior findings and advance the automated diagnoses of liver cancer, and also increase the accuracy and efficiency of diagnostics in research. In the same way, it is also suggested that these four resources would be utilised to gain a competitive advantage for the AI. community will also be able to expand the areas of greatest innovativeness of automated diagnosis, thereby increasing the precision and expandability of liver cancer diagnosis.

VIII. AI IN LIVER TUMOUR IMAGING

HCC and other liver tumors are notoriously difficult to differentiate. This challenge necessitates the use of advanced imaging modalities such as magnetic resonance imaging (MRI) and computed tomography (CT) for accurate diagnosis and effective treatment planning. Recent advances in artificial intelligence have significantly enhanced the analysis of liver tumors, particularly in tasks related to tumor segmentation, shape assessment, boundary detection, classification, and prognostic evaluation. Given the inherently complex nature of medical imaging, ranging from micrographs and CT scans to MRI sequences, there is a growing clinical demand for specialized, automated solutions leveraging deep learning and radiomics.

In this section, we systematically review AI-driven imaging approaches used in liver tumor analysis, structured based on imaging modality, technical complexity, and clinical utility. We begin with traditional segmentation techniques from CT scans (VIII.A), representing foundational clinical methods for delineating tumor boundaries. Subsequently, specialized imaging approaches such as perfusion mapping

and tumor characterization using CT are examined (VIII.B), offering functional insights into liver tumor vascularity and microcirculation that enhance diagnostic precision.

Advanced imaging and motion analysis techniques are discussed next (VIII.C), emphasizing solutions addressing tumor detection and characterization challenges caused by liver motion, a critical aspect in dynamic imaging contexts. Following this, diffusion-weighted MRI (DW-MRI) techniques for liver tumor characterization are explored (VIII.D), highlighting their role in providing enhanced tissue differentiation through advanced imaging contrasts. Comprehensive deep learning approaches are described (VIII.E), encompassing sophisticated methodologies that integrate earlier discussed techniques, showcasing a progression towards automated, precise, and clinically actionable AI-based diagnostic and segmentation systems.

We then highlight available radiology datasets specific to liver tumors (VIII.F), which are crucial resources for developing, validating, and benchmarking AI models, ensuring robust and generalizable performance. Finally, we provide an overview of state-of-the-art models (VIII.G), summarizing recent advancements and comparing their methodologies, dataset usage, and effectiveness in liver tumor analysis.

A detailed comparison of state-of-the-art deep learning architectures utilized for liver tumor segmentation across different imaging modalities is provided in Table 3, summarizing their network designs, datasets used, and key performance outcomes.

A. SEGMENTATION TECHNIQUES FOR LIVER TUMOURS FROM CT SCANS

Accurate segmentation of liver tumours from CT images is foundational to diagnosis, treatment planning, and therapy monitoring. Over the years, a variety of methods have been proposed, ranging from rule-based and probabilistic models to deep learning architectures. Each approach brings its own strengths and trade-offs, particularly in handling low contrast, tumor boundary irregularities, and inter-patient variability.

Qi et al. [63] introduced a semi-automatic method based on a Bayesian decision rule for segmenting liver tumors. Their technique involves manually selecting seed points and then employing a 3D Statistical Region (SR) growing strategy. Unlike earlier approaches that modeled tumor intensities using a single Gaussian distribution, they proposed a “bag of Gaussians” framework to better handle noise and intensity heterogeneity. This method demonstrated solid performance in the 3D Liver Tumour Segmentation Challenge 2008, with 87% accuracy and a Dice Similarity Coefficient (DSC) of 0.82. While the need for manual seeding limits full automation, this approach highlighted the power of probabilistic modeling in early segmentation tasks.

Kim et al. [64] developed a fully automatic method targeting both liver and HCC regions in CT scans. By leveraging both intensity distribution and morphological features, their model focuses on hypervascular tumors, which appear

brighter in contrast-enhanced CT. The method achieved 91% accuracy and a 93% true positive rate (TPR) compared to radiologist annotations, showing its potential as an auxiliary diagnostic tool, especially for early-stage HCC detection. However, its focus on hypervascular tumors might limit generalizability across broader tumor subtypes.

Abdel-Massieh et al. [65] proposed another automatic approach that relies on classical image processing techniques: contrast enhancement, Gaussian smoothing, and Isodata thresholding. These steps convert CT images into binary masks for tumor extraction. Their system reached 89% accuracy, 83% sensitivity, and 87% precision. Although simpler than learning-based methods, this approach offers a lightweight solution with relatively low computational demand, making it practical in resource-constrained settings. Yet, its performance may degrade on low-quality scans or atypical tumor presentations.

The emergence of deep learning has transformed liver tumor segmentation, offering end-to-end automation with enhanced accuracy. Almotairi et al. [66] adapted the SegNet architecture—originally designed for road scene segmentation—for liver tumor analysis by incorporating a VGG-16 encoder and a binary pixel-classification decoder. Their model achieved 99.9% accuracy and a DSC of 0.93. Key innovations include index-based upsampling to preserve boundary details, class weighting to address foreground-background imbalance, and robust data augmentation to handle imaging variability. This adaptation demonstrates the flexibility of generic architectures when appropriately tuned for medical contexts. However, the extremely high accuracy reported suggests the need for careful validation on external datasets to ensure model generalizability.

Gowda et al. [101] further advanced segmentation accuracy using a modified ResUNet architecture trained on the 3Dircadb dataset. Their pipeline incorporated intensity normalization, contrast enhancement, and extensive data augmentation. The model’s encoder utilized pretrained ResNet blocks for high-level feature extraction, while the decoder applied skip connections and upsampling for spatial refinement. They reported a DSC of 91.44% for liver and 75.84% for tumor segmentation—outperforming baseline UNet models. Additionally, the use of squeeze-and-excitation (SE) blocks and Atrous Spatial Pyramid Pooling (ASPP) allowed the model to focus on salient features and capture multi-scale contextual information. The implementation of Tversky loss also helped mitigate class imbalance—crucial when tumor regions are relatively small.

Despite promising results, Gowda et al. noted limitations such as high computational requirements and the risk of overfitting on limited training data. They advocated for future research to explore multi-phase imaging integration, larger datasets, and self-supervised learning to enhance model robustness and generalizability.

In summary, segmentation of liver tumors from CT has evolved from rule-based and probabilistic models to sophisticated deep learning pipelines. While early methods

laid the groundwork, modern architectures like ResUNet and SegNet derivatives offer superior performance, provided they are backed by diverse data and rigorous validation. The ongoing challenge remains balancing accuracy with generalizability and clinical feasibility.

B. PERFUSION MAPPING AND CHARACTERIZATION USING CT

Perfusion mapping using CT imaging provides a non-invasive means to quantify blood flow in liver tissues, offering functional insights that complement anatomical imaging. This modality has proven particularly valuable in characterizing liver tumors, where vascularity often correlates with tumor type, grade, and treatment response.

Tsushima et al. [67] used perfusion CT to analyze both HCC and metastatic liver tumors. Their method involved pixel-wise quantification to generate arterial and portal perfusion maps. They reported arterial perfusion values of 0.94 ± 0.26 mL/min/mL for HCC and 0.67 ± 0.33 mL/min/mL for colorectal metastases. With an 88% accuracy in distinguishing hypervascular lesions, the study demonstrated how perfusion CT can enhance tumor characterization by providing physiological information that augments traditional anatomical imaging. These findings underline perfusion CT's potential to improve treatment planning, particularly in differentiating tumor types that present similarly on standard scans.

In a retrospective analysis, Tan and Xiao [68] evaluated 54 cases of rare hepatic malignant tumors (HRMTs) using both CT and MRI imaging. By identifying characteristic imaging features specific to different tumor types, the study facilitated more precise diagnosis and staging of these rare malignancies. While significant overlap in imaging appearances exists, certain tumors exhibited distinguishable traits. The method achieved an identification accuracy of 82% and specificity of 79%, reinforcing the utility of dynamic and contrast-enhanced imaging in detecting diagnostically challenging lesions. However, the limited sample size and retrospective nature of the study suggest a need for validation on larger, prospective datasets.

Beyond traditional imaging, deep learning has increasingly been applied to automate and enhance liver tumor characterization in perfusion-related contexts. Tiraboschi et al. [92] developed three specialized U-Net-based models to segment the healthy liver (HL), metastatic liver area (MLA), and individual metastases (LM) in micro-CT images of pancreatic ductal adenocarcinoma (PDAC) mouse models. Their models achieved accuracy scores of 92.6%, 88.6%, and 91.5%, respectively, with Dice coefficients of 71.6%, 74.4%, and 29.9%. While segmentation of liver metastases (LM) lagged behind in performance, the overall results highlight the effectiveness of automatic methods in reducing manual workload and improving reproducibility. The relatively lower Dice score for LM, however, reveals the ongoing challenge in detecting small or low-contrast lesions, an area where

further refinement—such as attention mechanisms or post-processing refinements—could improve outcomes.

In a more advanced deep learning framework, Sun et al. [93] proposed RHEU-Net, a multi-scale liver tumor segmentation model based on a modified U-Net backbone. To enhance feature extraction, the traditional convolutional blocks were replaced with residual modules, stabilizing gradient flow and preserving low-level details. The model also introduced a Hybrid Gated Attention (HGA) module before the skip connections, enabling dynamic feature selection through channel and spatial attention mechanisms. Additionally, a Multi-Scale Feature Enhancement (MSFE) module using parallel atrous convolutions was integrated at the bottleneck layer to capture contextual information across different spatial resolutions. Evaluated on the LiTS2017 dataset, RHEU-Net achieved a Dice score of 95.72% for liver segmentation and 70.19% for tumor segmentation. These results are promising, indicating the model's capability to accurately delineate tumor boundaries, even in complex anatomical contexts. The integration of attention mechanisms and multi-scale processing addresses several traditional pitfalls in liver tumor segmentation, though the added complexity may pose challenges for real-time or low-resource clinical deployments.

CT-based perfusion mapping combined with modern deep learning models offers a powerful toolkit for liver tumor characterization. While traditional perfusion metrics provide critical physiological markers for tumor differentiation, AI-enabled models like RHEU-Net and U-Net variants enhance automation and precision. Future research should aim to bridge the gap between physiological interpretability and deep learning-based automation, ensuring models are not only accurate but also clinically explainable and deployable.

C. ADVANCED IMAGING TECHNIQUES AND MOTION ANALYSIS FOR LIVER TUMOR DETECTION AND CHARACTERIZATION

Advanced imaging plays a pivotal role in improving the detection and characterization of liver tumors, particularly in challenging scenarios where anatomical complexity, tumor heterogeneity, or motion artifacts impede accurate interpretation. This section discusses the application of state-of-the-art imaging modalities—CT, MRI, ultrasound, and cine-imaging techniques—and their interplay with motion-aware analysis to enable more precise and individualized diagnostics.

Ferrucci [69] offered a comprehensive evaluation of imaging modalities such as CT, MRI, ultrasound, and specialized techniques like CT during arterial portography (CTAP) for liver tumor assessment. While CT remains the gold standard in routine liver imaging with an approximate diagnostic accuracy of 90%, MRI has emerged as a superior modality in many contexts, particularly for lesions with complex vascularity or when radiation exposure must be minimized. MRI demonstrated up to 92% accuracy in liver tumor detection, making it a critical tool for

TABLE 3. Advanced Deep Learning Architectures for Liver Tumor Imaging. Each model is evaluated based on architecture, core innovations, validation datasets, and quantitative or clinical findings.

Model	Architecture / Approach	Key Features	Dataset / Validation	Performance / Findings
H-DenseUNet [108]	2D + 3D Hybrid Dense U-Net, cascaded (liver → tumor)	Intra-slice DenseNet and inter-slice features; ensemble used	LiTS 2017 (CT) Challenge	Achieved Dice of ~ 0.72 on LiTS; 2D/3D DenseNet ensemble improved volumetric continuity; strong performance but computationally heavy.
AH-Net [109]	Anisotropic Hybrid U-Net (2D encoder + 3D decoder)	2D convolutions for in-plane detail; 3D context in decoder	LiTS (CT), MRI dataset (ATLAS)	High liver Dice (~ 0.94) and good tumor surface agreement; joint segmentation on CT and MRI; effective feature integration but not tuned for small tumors.
nnUNet [110]	Auto-configuring U-Net (2D/3D)	Self-configures preprocessing and hyperparams per data	LiTS (CT), CHAOS (MRI), etc.	~95% liver Dice on CT, ~75% on MRI; benchmark model; generalizes well but tumor performance varies with lesion size and dataset quality.
Attention U-Net [111]	U-Net + Attention Gates	Focuses on relevant regions by gating skip connections	LiTS (CT) and other medical images	Improved tumor segmentation over vanilla U-Net; commonly used as an attention mechanism baseline; lacks global context modeling.
TransUNet [112]	U-Net + Vision Transformer encoder	Combines ViT for encoding with U-Net decoder	Synapse multi-organ (CT), applied to LiTS	First ViT-CNN hybrid in medical imaging; strong multi-organ performance; captures long-range context but requires large datasets and compute.
Swin UNETR [113]	Fully transformer-based U-Net (Swin Transformer backbone)	Hierarchical Swin Transformer encoding + CNN decoder	BTCV, LiTS (CT); CHAOS (MRI)	Dice ~0.82–0.89 on MRI; effective in organ segmentation; underperforms CNNs on tumor segmentation unless trained on large-scale data.
CAFCT-Net [114]	CNN-Transformer Hybrid U-Net	Attentional feature fusion, ASPP module, Transformer layers	LiTS 2017 (CT)	Dice 84.3%, IoU 76.5%; outperformed Attention U-Net and PVT-Former; excels at boundary precision; moderate training complexity.
HyborNet [115]	Dual-branch Conv + Swin Transformer network	Gabor conv attentions for edges; cross-attention fusion; deep supervision	Private dataset (CT) + LiTS-like task	Outperformed SOTA baselines; strong on small and irregular lesions due to Gabor attention and cross-branch fusion.
AC-Net [116]	U-Net variant with Axial & Transformer Attention	Axial attention in skip connections; Transformer at bottleneck	LiTS (CT) + Hubei Hospital (CT & MRI)	Dice 0.90 (CT), 0.80 (MRI); robust to modality shifts; attention-based skip connections improved generalizability across CT and MRI.
MI-TransSeg [117]	Multi-phase Transformer Network	Learns interactions between arterial & venous CT phases	Multi-phase CT (research dataset)	Fused arterial and venous contrast phases for joint tumor + MVI prediction; outperformed single-phase baselines; strong temporal-context learning.
Diff4MMLiTS [118]	Diffusion-based Multimodal Pipeline	Synthesizes aligned CT pairs with and without tumor across modalities for training	LiTS (CT) + Internal multi-phase CT	Improved segmentation without aligned paired scans; uses synthetic multimodal training data; performance better than prior multimodal approaches.
Selective Ensemble [119]	Two-model ensemble (ConvNeXt U-Nets)	One model for all lesions, one specialized for small lesions; selects best mask	LiTS (CT), KiTS (CT), VinDr-Liver (CT)	Selective inference boosted small lesion detection; improved total lesions found vs. single models; reduced false negatives.
Multi-dataset Learner [120]	Domain-generalized nnUNet pipeline	Pseudo-labeling + self-ensemble + CycleGAN translation to use external data	MRI (CHAOS, private, etc.)	Liver Dice 95.7%, tumor Dice 72.2% on unseen MRI; robust to domain shifts; outperformed 92%/68% baseline.
InferVision AI [121]	Coarse-to-fine pipeline (3D ResUNet)	Multi-center external validation; real-world clinical usage	Multi-center CT cohort (HCC patients)	Dice ~0.88 for tumors; generalizes well in clinical HCC cases; surpasses earlier AI benchmarks (Dice ~0.75–0.85).

cases requiring detailed soft tissue contrast and vascular mapping. The authors emphasized that imaging modality selection should not be uniform but rather guided by clinical context—including tumor type, liver function, and staging needs. This underscores a shift in liver oncology toward precision imaging strategies tailored to individual patient profiles.

In the pediatric domain, Vasireddi et al. [70] explored the diagnostic role of MRI in evaluating pediatric liver tumors such as vascular tumors, hepatoblastoma, and fibrolamellar hepatocellular carcinoma. They highlighted how hepatobiliary contrast agents, particularly gadoxetate disodium, improve lesion visibility and tissue differentiation in developing livers. Despite the challenge of overlapping imaging characteristics among tumor types, the authors noted that certain morphological features—such as internal septations, necrotic zones, and enhancement kinetics—can guide differential diagnosis. The study also outlined MRI-based diagnostic protocols that assist radiologists in distinguishing benign from malignant entities, where accuracy is crucial given the limited treatment window in pediatric oncology. Their work reflects a growing interest in

integrating functional contrast enhancement with AI-assisted interpretation to improve diagnostic consistency in pediatric populations.

Motion analysis is a particularly critical consideration in liver tumor detection due to respiratory-induced liver displacement. Kirilova et al. [71] conducted a detailed investigation into liver tumor motion using cine-MRI, quantifying tumor displacements across multiple planes. The average craniocaudal motion was 15.5 mm, with anteroposterior and mediolateral shifts of 10 mm and 7.5 mm, respectively. Importantly, the study found no consistent correlation between diaphragm movement and tumor displacement, debunking a common surrogate marker assumption in motion modeling. These findings have substantial implications for radiotherapy planning, particularly in SBRT, where millimeter-level accuracy is required. The authors advocate for patient-specific motion profiling to guide dose delivery and tumor tracking, highlighting the role of advanced imaging not only in diagnosis but also in therapy optimization. The study's reported intraobserver error of under 2 mm supports the reliability of cine-MRI for such applications, though it also introduces the need for

increased imaging infrastructure and planning time in clinical settings.

In the domain of real-time and accessible imaging, Nishida and Kudo [72] evaluated the use of artificial intelligence in ultrasound-based liver tumor detection. Ultrasound, though cost-effective and widely available, suffers from operator dependency and low reproducibility due to inconsistent acquisition conditions. The authors discussed how CNNs have been trained to recognize patterns in liver lesions, including HCC, liver cysts, and metastatic tumors. They reported that in several settings, AI approaches are nearing radiologist-level performance in classifying liver lesions. While the paper did not provide explicit numerical metrics, it provided a valuable overview of how CNNs can help standardize interpretation in low-resource environments. A major takeaway is that the application of AI in ultrasound is not just about automating diagnosis but also about democratizing access to expert-level decision support. However, the success of such models depends heavily on high-quality, diverse datasets and standardized image acquisition protocols—factors that remain bottlenecks in real-world adoption.

The integration of advanced imaging modalities with motion analysis and artificial intelligence is redefining liver tumor diagnostics. Static imaging techniques like CT and MRI provide anatomical detail, while dynamic imaging methods such as cine-MRI offer crucial insights into tumor movement—especially relevant for image-guided interventions. Meanwhile, AI applications in modalities like ultrasound are beginning to bridge the gap between high accuracy and global accessibility. Moving forward, the fusion of multi-modal imaging, real-time motion compensation, and AI-driven interpretability will be key to delivering accurate, efficient, and equitable liver cancer care.

D. DIFFUSION-WEIGHTED MRI (DW-MRI) FOR LIVER TUMOR CHARACTERIZATION

Chan et al. [73] used diffusion-weighted morphology (DW-MRI) to differentiate hepatic abscesses from cystic or necrotic tumours. The study used apparent diffusion coefficient (ADC) values; hepatic abscesses had a mean ADC value of $0.67 \pm 0.35 \times 10^{-3} \text{ mm}^2/\text{s}$, whereas cystic or necrotic tumours had significantly higher ADC values ($p < 0.0001$), $2.65 \pm 0.49 \times 10^{-3} \text{ mm}^2/\text{s}$. This differentiation is important for determining appropriate treatment strategies. Results showed that DW-MRI can well discriminate between these types of liver lesions, and ADC values can yield substantial differentiation accuracy between the disease regions.

Wagner et al. [74] characterized liver tumours based on DW-MRI to distinguish between regions of viable, fibrous, and necrotic tumour. Viable tumour regions showed significantly different pure diffusion coefficients ($1.16 \pm 0.29 \times 10^{-3} \text{ mm}^2/\text{s}$) compared with necrotic regions ($1.70 \pm 0.49 \times 10^{-3} \text{ mm}^2/\text{s}$) and a lower perfusion fraction than in viable regions ($14\% \pm 6\%$ vs. $21\% \pm 8\%$). These results demonstrate that DW-MRI can effectively separate these regions for treatment planning purposes.

E. DEEP LEARNING APPROACHES FOR LIVER TUMOUR DIAGNOSIS AND SEGMENTATION

Recent advancements in DL have significantly improved the ability to automatically diagnose and segment liver tumors with high accuracy and generalizability. These models capitalize on their ability to learn hierarchical image features and patterns from large volumes of data, thereby automating tasks traditionally reliant on radiologist interpretation. While early CNN architectures laid the groundwork for medical imaging automation, the field has since expanded into hybrid networks, multi-modal integration, radiomics-guided pipelines, and biologically inspired frameworks.

Zhen et al. [75] developed a deep learning system that integrated MRI sequences with comprehensive clinical data to classify liver tumors accurately. Leveraging a modified Inception-ResNet V2 network pretrained on ImageNet, the model combined six MRI sequences or a reduced set of three non-enhanced sequences (T2-weighted, DWI, and pre-contrast T1-weighted) with clinical variables such as tumor markers and liver function results. The inclusion of clinical information in the model's fully connected layers substantially improved classification performance. Their model achieved an AUC of 0.985 for HCC classification with a sensitivity of 91.9%, while still maintaining strong diagnostic performance using only non-contrast sequences. Saliency maps were used to highlight attention on diagnostically critical regions, increasing interpretability and clinician trust. This study underscores the value of hybrid models that fuse imaging and non-imaging data, particularly in contrast-free scenarios or resource-limited settings.

Goehler et al. [76] explored 3D neural networks for liver metastasis detection and tracking across MRI follow-ups. Their ResNet-18—based U-Net architecture could not only detect liver lesions but also assess interval changes in tumor burden between scans. Achieving 91% agreement with radiologists on lesion progression and Dice coefficients between 0.73 and 0.81 for lesion segmentation, the system shows promise in longitudinal tumor monitoring. Importantly, these tools provide radiologists with supplementary quantitative data that may improve decision-making in treatment response evaluations.

Hendi et al. [95] proposed a hybrid CNN+LSTM framework for liver disease subtyping and progression prediction. By combining spatial image processing capabilities of CNNs with the sequential modeling strengths of LSTMs, the model captured both anatomical patterns and temporal dependencies. With performance metrics including 98.73% accuracy, 99% precision, and 99% AUC-ROC, this method outperformed traditional CNNs, RNNs, and standalone LSTMs. While the model proved robust, its computational complexity and dependence on large, diverse datasets highlight the need for further scalability and external validation. Moreover, the authors emphasized the potential of integrating multi-modal data (CT, MRI, genomics) to enhance disease modeling.

Jumaah et al. [96] introduced the Artificial Liver Classifier (ALC), a supervised learning model inspired by the liver's

natural detoxification mechanism. Designed without hyperparameters and optimized using an Improved FOX (IFOX) metaheuristic, ALC offered both simplicity and strong performance, achieving 100% accuracy on the Iris dataset and over 99% on Breast Cancer and other benchmarks. While ALC showcases the promise of biologically inspired and hyperparameter-free models, its validation on real-world liver imaging datasets remains pending. Nevertheless, it highlights a growing research interest in lightweight, scalable classifiers that reduce overfitting and training overhead.

Zossou et al. [97] also explored CNN+LSTM architectures for liver disease prediction and subtyping. Echoing the findings of Hendi et al., their model achieved 98.73% accuracy and demonstrated strong generalization across modalities. Notably, the work supports the broader trend toward leveraging temporal patterns and multi-modal fusion to improve diagnostic precision. However, like many such models, it faces challenges in training efficiency and access to curated multi-center datasets.

Mocan et al. [98] introduced a segmentation-classification pipeline using a Coot Optimization Algorithm—based Extreme Learning Machine. Their method integrated feature selection and parameter tuning to minimize overfitting while maintaining high accuracy. With 97.85% accuracy and an AUC-ROC of 98.1%, the model outperformed conventional methods like SVMs and Random Forests. This optimization-guided learning demonstrates how nature-inspired metaheuristics can fine-tune deep models, though it also raises concerns about computational cost and cross-institutional generalizability.

Radiomics-guided approaches are also gaining traction. Granata et al. [99] combined hepatospecific contrast-enhanced MRI with radiomics feature extraction to predict tumor budding in colorectal liver metastases. Using 3D Slicer for segmentation and PyRadiomics for feature computation, they evaluated multiple classifiers, with KNN achieving the best performance—95% accuracy and 0.96 AUC. The model demonstrated strong validation metrics (94% accuracy and 95% specificity) on external cohorts. This reinforces the clinical value of combining radiomics and ML in preoperative risk stratification. However, the need for standardized radiomics protocols remains a key bottleneck for widespread adoption.

Recent research has also advanced the architectural frontier through hybrid CNN-transformer designs and ensemble-based systems. Notable examples such as HyborNet, CAFCT-Net, and AC-Net have demonstrated improvements in segmentation accuracy by combining the spatial inductive bias of CNNs with the global context awareness of transformers. These models excel in complex segmentation tasks, particularly when lesion boundaries are irregular or contrast is limited. Their success suggests that the future of liver tumor segmentation may lie in carefully balanced architectures that unify local and global representation learning.

Deep learning applications in liver tumor diagnosis and segmentation have evolved from simple CNNs to sophisticated,

context-aware architectures incorporating attention mechanisms, multi-modal fusion, biologically inspired learning, and explainable AI. While the performance of these systems is impressive, challenges such as computational demands, dataset diversity, real-world validation, and clinical integration remain. Future directions should focus on collaborative benchmarking, integration of radiomics-genomics-imaging pipelines, and transparent model interpretability to enhance trust and facilitate deployment in diverse clinical environments.

1) HYBRID CNN-TRANSFORMER MODELS FOR LIVER TUMOR SEGMENTATION

Recent advancements in medical image segmentation have increasingly focused on hybrid deep learning models that combine CNNs with Transformer-based architectures. These hybrid designs aim to leverage the strengths of CNNs in capturing fine-grained local features and the global contextual modeling capabilities of Transformers. In liver tumor segmentation, where both sharp lesion boundaries and holistic anatomical context are essential, such architectures have shown substantial promise.

HyborNet (Hybrid Gabor Attention Convolution and Transformer Network) [115] exemplifies this trend through a dual-branch encoder architecture. One branch is a CNN enhanced with Gabor attention modules, specifically tuned for edge-aware feature extraction and capturing detailed local textures. The second branch integrates a Transformer backbone to encode global spatial dependencies, enabling the model to reason about tumor context across the entire liver region. These branches are fused using a cross-attention module, which dynamically integrates local and global features. A hierarchical deep supervision mechanism is also employed to refine intermediate outputs and guide multi-scale learning. Evaluation results demonstrated that HyborNet significantly outperforms previous state-of-the-art segmentation models, highlighting the value of combining convolutional precision with transformer-based contextualization.

CAFCT-Net (Contextual and Attentional Feature-fusion CNN-Transformer Network) [114] is another representative hybrid framework that integrates atrous spatial pyramid pooling (ASPP), attention gates, and Transformer components into a U-Net-like architecture. The model introduces an Attentional Feature Fusion (AFF) module to adaptively combine multi-scale features from CNN and Transformer paths. When tested on the LiTS (Liver Tumor Segmentation) public dataset, CAFCT-Net achieved a Dice Similarity Coefficient of approximately 84.3% and an Intersection over Union (IoU) of 76.5%, surpassing both conventional CNN models like Attention U-Net and pure Transformer-based models such as PVT-Former. This demonstrates that synergistically blending local detail and long-range dependency modeling can yield more robust and accurate tumor segmentation outcomes.

AC-Net [116] further explores this hybrid paradigm by adapting a 3D U-Net backbone for multi-modal tumor segmentation, integrating two key attention modules. First,

the Axial Attention Module replaces traditional skip connections to better capture inter-slice spatial dependencies in volumetric data. Second, a Vision Transformer Module is embedded in the network bottleneck to encode global image features across slices. The model was pretrained on the LiTS dataset (CT scans) and subsequently fine-tuned using a proprietary hospital dataset containing both CT and MRI images. Impressively, AC-Net achieved a Dice score of 0.90 on CT and 0.80 on MRI tumor segmentation tasks, demonstrating its adaptability across modalities. The attention-based skip connections were shown to significantly enhance segmentation accuracy, particularly in the presence of complex anatomical variability and low-contrast lesions common in MRI scans.

These hybrid architectures represent a compelling step forward in liver tumor segmentation, combining the inductive biases of CNNs with the expressive power of Transformers. While these models show strong quantitative performance, future work should continue to address challenges such as computational efficiency, interpretability, and real-time deployment feasibility—particularly for use in clinical workflows where both accuracy and speed are essential.

2) ENSEMBLE APPROACHES TO IMPROVE SEGMENTATION ACCURACY

Ensembling is a widely adopted strategy in medical image segmentation for improving model robustness, reducing variance, and capturing complementary strengths of different architectures or training paradigms. Rather than relying on a single network, ensemble-based approaches integrate multiple model outputs—either through averaging, voting, or hierarchical coordination—to achieve better generalization and mitigate the risk of missed detections. Recent studies in liver tumor segmentation have demonstrated the versatility of ensembling, particularly in detecting small lesions, improving boundary precision, and handling intra-class variability.

- **Multi-model Ensembles:** Multi-model ensembles, such as the approach by Al-Battal et al. [119], demonstrate the power of combining specialized and generalist models. They trained two ConvNeXt-augmented U-Net variants—one designed to segment all hepatic tumors and another focused specifically on small lesions. During inference, both models generated segmentation masks, and a contrast-based selection mechanism chose the more confident result for each region. This dual-model ensemble improved the detection of subtle hepatic lesions, which are frequently missed by monolithic networks, and increased the total number of tumors identified across three independent liver and kidney tumor datasets. The use of a specialist model specifically tailored for small lesion detection is a practical response to the class imbalance challenge common in clinical datasets, where large tumors dominate and smaller ones are often underrepresented in model training. This approach also underscores the clinical relevance of sensitivity enhancement without sacrificing specificity.

- **Ensembling by Different Initializations:** Ensembling by different initializations, as explored by Xie et al. [122], takes a simpler but effective route by training multiple instances of the same architecture using different random seeds. These independently trained models capture slightly different decision boundaries due to stochastic training processes. At inference, their outputs are averaged to reduce overfitting and smooth out idiosyncratic prediction errors. The ensemble led to significantly improved segmentation stability across a range of liver tumor types. Notably, this method avoids the computational overhead of designing entirely different architectures while still benefiting from diversity through training variance. The strategy highlights how ensembling—even within architectural constraints—can produce measurable gains in robustness and reproducibility.
- **Two-Stage (Coarse-to-Fine) Models:** Two-stage (coarse-to-fine) pipelines, while not traditional ensembles of parallel models, can be viewed as sequential ensembles that build upon each other. An example is the commercial liver tumor segmentation system developed by Shan et al. [121] for InferVision. Their pipeline employs a 3D ResUNet in the first stage to perform coarse localization of lesion regions, followed by a fine-stage model that refines tumor boundaries. The initial stage provides spatial priors that guide the second stage, which improves granularity and reduces false positives. This hierarchical refinement strategy achieved a Dice coefficient of 0.88 on external validation, demonstrating strong performance in generalizing to unseen data. Importantly, this architecture mimics clinical reasoning—first detecting an area of interest and then applying more focused analysis—making it intuitively appealing and effective. The success of this pipeline showcases how cascading models can balance sensitivity and precision in a clinically meaningful way.

3) MULTI-MODAL IMAGING INTEGRATION (CT, MRI, etc.)

Integrating information from multiple imaging modalities can provide a more comprehensive analysis of liver tumors. Multi-modal fusion approaches have been developed to exploit the complementary information available from CT, MRI, or multi-phase scans. For instance, Chen et al. [118] introduced Diff4MMLiTS—a four-stage pipeline for multimodal liver tumor segmentation—that eliminates the need for perfectly aligned dual-modality images. Their approach synthesizes aligned multimodal data using a latent diffusion model by registering organs across modalities, removing tumors from one modality via in-painting, and then generating a corresponding tumor appearance in the other modality. The segmentation network is trained on these paired synthetic images, resulting in superior performance over traditional multimodal segmentation methods. This diffusion-based data augmentation offers a promising way to fuse modalities for tumor analysis.

TABLE 4. Radiology Datasets for Liver Tumour (Part 1).

Dataset	Image Format	Task	Description
LiTS	CT	Liver and Tumour Segmentation	<ul style="list-style-type: none"> Annotation Protocol: Multiple radiologists manually segmented both liver and lesions; final consensus masks used. No official inter-observer metric (e.g., kappa) published. Tumor Subtypes: Primarily HCC, some metastatic lesions. Imaging Inconsistencies: Contrast-enhanced CT from multiple institutions, varying scanner parameters. Notes/Limits: Class imbalance often skews toward HCC; widely used in challenges (e.g., ISBI, MICCAI). Overlaps partially with other public CT sets.
Medical Segmentation Decathlon (MSD)	CT	Liver and Tumour Segmentation	<ul style="list-style-type: none"> Annotation Protocol: Expert annotations (1–2 radiologists); no public inter-observer agreement statistics. Tumor Subtypes: Task 3 focuses on liver tumours (HCC, possible metastases). Imaging Inconsistencies: Single-/multi-phase CT from various centers; differences in resolution, contrast timing. Notes/Limits: Large, diverse dataset for benchmarking. Often used in competitions; can reveal domain shift issues due to multi-center data.
3D-IRCADb	CT	Liver and Tumour Segmentation	<ul style="list-style-type: none"> Annotation Protocol: Single radiologist or small expert team; no consensus labeling or inter-observer metric. Tumor Subtypes: Includes normal liver, HCC, and some metastases. Imaging Inconsistencies: Contrast-enhanced CT from a single center; standardized protocol but small sample (20 patients). Notes/Limits: Often used for proof-of-concept. Limited external validity due to small size; no official multi-radiologist cross-check.
CHAOS (Combined Healthy Abdominal Organ Segmentation)	CT, MRI	Liver Segmentation	<ul style="list-style-type: none"> Annotation Protocol: Multi-organ ground-truth from radiologists; no standardized multi-radiologist metrics reported. Tumor Subtypes: Primarily healthy liver; limited tumor cases (rare subtypes not emphasized). Imaging Inconsistencies: Various MRI sequences (T1, T2) and CT phases; multi-center differences in scanning parameters. Notes/Limits: Focus on normal-liver segmentation. Scanner diversity can complicate model training; not primarily a tumor dataset.
NIH Pancreas Dataset	CT	Abdominal Organ Segmentation	<ul style="list-style-type: none"> Annotation Protocol: Single radiologist or small team; no inter-observer metric published. Tumor Subtypes: Mainly for pancreas, partial liver coverage. Rarely includes explicit liver tumor labels. Imaging Inconsistencies: Contrast-enhanced CT with varied phases; single center (NIH). Notes/Limits: Not dedicated to liver tumours; class imbalance if used for partial liver segmentation.

In a related strategy, Zhao et al. [120] proposed MI-TransSeg, a multi-phase feature interaction Transformer network that processes contrast-enhanced CT images acquired in different phases. By jointly learning from arterial and venous phase images, the model is better able to delineate tumors that appear differently across phases, thereby improving accuracy in capturing tumor extent and even detecting signs of microvascular invasion. Furthermore, the AC-Net model

exemplifies training on both CT and MRI; by pretraining on a large CT dataset and fine-tuning on MRI, the network effectively learns modality-invariant features. This allows it to segment liver lesions on MRI with approximately 80% Dice, even though it was originally developed on CT, suggesting that shared-feature representations can enable a single model to operate across different modalities when simultaneous input fusion is not feasible.

TABLE 5. Radiology Datasets for Liver Tumour (Part 2).

Dataset	Image Format	Task	Description
HepaBIG Dataset	MRI	Liver Tumour Segmentation	<ul style="list-style-type: none"> Annotation Protocol: Manual MRI annotations by expert radiologists; no consensus or inter-observer stats. Tumor Subtypes: Mostly HCC; possible additional subtypes not well-documented. Imaging Inconsistencies: 1.5T or 3T MRI; multi-phase sequences (arterial, venous). Potential motion artifacts in dynamic imaging. Notes/Limits: Often requires direct contact with dataset creators. Good for advanced MRI-based tumor analysis but lacks large-scale multi-center diversity.
CLiver Dataset	CT	Liver Tumour Segmentation	<ul style="list-style-type: none"> Annotation Protocol: Manual segmentation by experienced radiologists; no published inter-observer metrics. Tumor Subtypes: Various tumor types (HCC, metastases). Imaging Inconsistencies: Single- or multi-phase CT from a single center; uniform scanning protocol but limited patient variety. Notes/Limits: Common for evaluating segmentation methods; smaller than LiTS or MSD.
TCIA (The Cancer Imaging Archive) - Liver	CT, MRI	Liver Tumour Segmentation	<ul style="list-style-type: none"> Annotation Protocol: Different institution-provided annotations; sometimes single radiologist, sometimes multi-radiologist (depends on the specific collection). Tumor Subtypes: Multiple subtypes (HCC, metastases, rare lesions) from various scanners. Imaging Inconsistencies: 1.5T/3T MRI, multi-phase CT, multi-center. Potential scanner variation and protocol mismatch. Notes/Limits: Free access; multi-center data fosters generalizability but requires robust domain adaptation.
MICCAI	Varying (CT)	Liver and Tumour Segmentation	<ul style="list-style-type: none"> Annotation Protocol: Ground-truth often by 2–3 radiologists; no uniform inter-observer metric across different MICCAI challenges. Tumor Subtypes: Typically HCC and metastases. Some tasks focus on other abdominal organs. Imaging Inconsistencies: Multiple phases or single-phase CT, multi-center. Variation in slice thickness, contrast usage. Notes/Limits: Annual challenges with training/validation sets. Labeling consistency can differ across tasks.
SegTHOR Dataset	CT	Organ Segmentation	<ul style="list-style-type: none"> Annotation Protocol: Provided by trained experts; no multi-radiologist data or inter-observer metric. Tumor Subtypes: Focuses on thoracic organs; liver coverage is minimal/adjacent, not tumor-specific. Imaging Inconsistencies: Single-phase CT from a single center; consistent scanning protocol but limited data volume. Notes/Limits: Not dedicated to liver tumor tasks. Partial liver included for multi-organ segmentation context.

4) SWIN TRANSFORMER VERSUS CNN: COMPARATIVE STUDIES

Transformers, especially vision transformers like the Swin Transformer, have been proposed as alternatives to traditional CNN backbones for medical imaging. Hatamizadeh et al. [113] conducted a rigorous comparison between a Swin-UNETR (a transformer-based U-Net) and established CNN-based models such as nnUNet and a parameter-efficient

“PocketNet” variant for liver segmentation on MRI. The study found that classic CNN models outperformed the Swin Transformer approach in a multi-institutional dataset, with CNN-based architectures achieving Dice scores in the range of 0.92–0.95 compared to 0.82–0.89 for the Swin-UNETR. The higher variance and the susceptibility of the transformer-based model to artifacts suggest that, in scenarios with limited training data or high noise, CNNs—with their

strong inductive biases—can generalize more effectively. Conversely, hybrid models that integrate Swin Transformer modules with CNN components, such as CAFCT-Net, have shown superior performance by leveraging both global context and precise localization. This indicates that while pure transformer-based models may require very large datasets or additional regularization, combining them with CNN layers can lead to improved segmentation outcomes in practical clinical settings.

5) DOMAIN ADAPTATION AND GENERALIZATION ACROSS DATASETS

A critical focus of recent research has been enhancing model generalization across different data sources, hospitals, and imaging protocols through domain adaptation techniques. Zhao et al. [120] addressed the challenge of limited labeled MRI data by aggregating multiple datasets and incorporating unlabeled data via pseudo-labeling and unpaired image-to-image translation. They further applied a self-ensemble learning strategy, augmenting test-time predictions through multiple perturbed versions of the model, which boosted average Dice scores from 92% to 95.7% for liver segmentation and from 68% to 72.2% for tumor segmentation on target MRI sets. In another study, Yang et al. [123] proposed an unsupervised domain adaptation (UDA) framework that adapts models from CT to MRI (and vice versa) without requiring target labels. Their approach enhances feature alignment between domains using cross-pseudo supervision, wherein two segmentation networks are trained simultaneously on source and target data, with each network's predictions serving as pseudo-labels for the other. A self-attention module within the feature-aligner ensures that structurally relevant features are matched across modalities.

6) EXTERNAL VALIDATION AND CLINICAL EFFICACY STUDIES

For AI models to be successfully integrated into clinical practice, rigorous external validation on real-world data is essential. Shan et al. [121] performed an independent multi-center validation of an AI-assisted HCC segmentation platform on CT scans. Developed by Infervision, China, this system utilized a 3D ResUNet-based model and was tested on cases from hospitals not included in the training data, achieving an average Dice score of 0.882 in delineating liver tumors. Notably, for larger tumors (greater than 2 cm), Dice scores exceeded 0.90, and performance was consistent across different tumor locations, outperforming earlier published methods that reported Dice scores of approximately 0.75–0.85.

F. RADIOLOGY DATASETS OF LIVER TUMOUR

Liver tumor radiology datasets are essential resources for the development and validation of AI models in medical imaging. These datasets provide a rich collection of liver scans using modalities such as CT and MRI, which are

crucial for training machine learning algorithms in tasks like liver tumor detection, segmentation, and classification. High-quality annotated datasets allow researchers to fine-tune their models, ensuring accuracy in clinical diagnosis and treatment planning. By offering standardized imaging data, these datasets help to drive innovation in liver tumor research, enabling more accurate and efficient AI-driven solutions in radiology. Table 4. summarizes the various liver tumor datasets currently available, detailing their imaging modalities, annotation types, and specific applications.

G. STATE-OF-THE-ART MODELS

The introduction of state-of-the-art models, including deep learning algorithms such as CNNs, transformers, and hybrid optimization techniques, has revolutionized liver tumour analysis. These models not only enhance the accuracy of segmentation but also support predictive analytics, such as mutation prediction and survival analysis. In this section, we explore a range of cutting-edge models and methodologies developed to address the challenges of liver tumor classification, segmentation, and prognosis. Each model leverages sophisticated pre-processing techniques, publicly available datasets, or proprietary clinical data, and delivers quantifiable results that demonstrate advancements in the field. Table 5. provides a detailed overview of key models, their applications, and performance metrics, along with a discussion of their methods, contributions, and limitations.

IX. LIVER TUMOUR GROWTH RATE AND SURVIVAL ANALYSIS

Liver tumour growing time is highly relevant in the determination of the survival advantage of any patients with liver cancer as well as the management strategies to be used. Thus, by using quality images, models with animals and cadavers and comparing them with clinical cases, growth profiles of tumours, rates of recurrence and overall survival have been determined for usage in clinical practice. This section presents reviews of results concerning the analysis of the various aspects of tumour growth kinetics, histopathologic growth prediction, and survival and surgical management of liver metastases.

A. TUMOUR GROWTH PATTERNS AND RECURRENCE ANALYSIS

Pinheiro et al. [77] studied on relationship of tumour growth patterns in recurring CRLM following surgical resection. According to the 91 patients of each group; pathological specimens were characterized either as infiltrative type or pushing type. The findings of this study revealed that the recurrent rate was at 71.4%, and the following features as independent predictors of the recurrence: three or more lesions, and an infiltrative margin. The disease-free survival rate at 5 years in relation to the pushing margins was 40.5% and for infiltrative margins was 20.2% ($P = 0.05$). These results indicate that tumour margin patterns are

TABLE 6. Different State-of-The-Art models.

Reference	Application	Pre-processing	Dataset	Result, Methods, Contributions, and Limitations
[57]	Liver and tumor segmentation	Contrast enhancement, noise reduction	LiTS dataset	Dice: 0.967 (liver), 0.725 (tumour). Two-stage CNN model with liver localization and tumor segmentation. Attention mechanism improves small tumor detection. Limitation: Minor segmentation errors for small tumours.
[58]	Liver tumor segmentation and classification	Contrast improvement via histogram equalization, median filtering for noise reduction	MICCAI SLiver'07, 3 Dircadb01, and LiTS	Segmentation Dice: 0.85. APESTNet with Mask R-CNN and Swin Transformer for feature extraction and classification. Limitation: Prone to over/under-segmentation at boundaries.
[59]	Treatment prediction, survival analysis	Image segmentation, feature extraction via Gray-level Co-occurrence Matrix (GLCM)	72 patient CT scans Private dataset	Prediction accuracy: 86%. Uses texture features to predict survival outcomes using SVM. Limitation: Limited dataset size.
[60]	Liver lesion segmentation and classification	SegNet for liver segmentation, UNet for lesion extraction	LiTS dataset	Segmentation Dice: 0.92. Combines SegNet, UNet, and bio-inspired artificial bee colony optimization for feature selection. Limitation: Complex model training process.
[61]	Liver tumour classification	Haar wavelet transform for feature extraction	Private Liver cancer dataset	Accuracy: 99.41%. GWO-ELM model acts as an SVM-like classifier with high efficiency. Limitation: Generalization to other datasets not tested.
[62]	Tumour segmentation and classification	Histogram equalization, anisotropic diffusion filtering	LiTS dataset	Segmentation Dice: 0.88. Uses optimized fuzzy centroid region growing with salp swarm optimization. Limitation: Restricted generalizability beyond CT images.
[50]	Automatic diagnosis of sub-types of liver HCC	H&E stained liver histopathology image processing	KMC and TCGA-Liver datasets	Accuracy: 90.93% (KMC dataset), 97.72% (TCGA-Liver dataset). LiverNet deep learning architecture classifies liver tissue into normal and HCC sub-types. Outperforms state-of-the-art models with fewer parameters and computational requirements.
[51]	Nuclei segmentation of liver cancer histopathology images	Image preprocessing with robust residual block and modified attention mechanism	Kumar dataset and KMC dataset	F1 and Jaccard Index (JI) improved by 3% on KMC dataset and over 1% on Kumar dataset. NucleiSegNet addresses shape variability and nuclei touching issues, improving spatial information extraction and leveraging salient features with only 13 million parameters. It outperforms other models in accuracy and computational efficiency.

prognosticator of disease-free survival for patients and may assist in identifying patients for further adjuvant treatment.

B. RADIOMICS FOR PREDICTING HISTOPATHOLOGIC GROWTH PATTERNS

Radiomics has recently been identified as a potential method to predict HGP in liver tumours and to non-invasively characterize tumours for better planning of the treatment. In patients with CRLM treated with bevacizumab-containing chemotherapy, Wei et al. [78] constructed a radiomics model to differentiate desmoplastic from replacement pattern lesions. For lesion based and the patient based results, the model attained the AUCs of 0.707 and 0.720, respectively. When applied in guiding the choice of treatment strategies for patients with desmoplastic growth, the model accurately predicted that the 1-year PFS of patients with this histological pattern was significantly higher than the PFS of the other patients.

Cheng et al. [79] proposed a radiomics process to come up with a non-invasive *in vivo* imaging method to evaluate HGP in CRLM using contrast-enhanced MDCT images. The accuracy of the model was further reflected by an AUC of 0.926 and AUC of 0.939 in the training and validation sets respectively to characterise tumour growth kinetics. Latacz et al. [80] assessed if HGPs can be found in liver metastases with medical imaging. In work we also outlined the ability to use radiomic models in CT or MR images for the identification of high-efficiency HGPs. This approach could help in organizing the patient's therapy according to the biological nature and the rate of metastases' growth. For all such data, a multicentre trial is needed.

C. INFLUENCE OF TUMOUR GROWTH RATE ON SURVIVAL OUTCOMES

Hanouneh et al. [81] aimed at evaluating tumour growth rate and HCC recurrence in a series of LTs in patients outside Milan or UCSF criteria. The overall patient death rate was too low to discern trends, but patients with a tumour growth rate $\leq 1.61 \text{ cm}^3/\text{month}$ had a significantly lower mean recurrence of 11% compared to 58% in patients with higher tumour growth rates ($P = 0.023$), respectively.

This raises the possibility that the rate of tumour growth can indeed be used as the framework by which LTs can be chosen from patients that fall outside the traditional scoring criteria.

Barbara et al. [82] also evaluated growth patterns and survival in 39 patients with untreated small HCC and cirrhosis. The study identified three growth patterns: Slow growth, declining growth rate, and constant growth rate. Scoring system elaborated with analysis of albumin, alcohol use, and number of nodules to predict tumour doubling time. The estimated survival probabilities were 0.81 at year 1, 0.557 at year 2, 0.21 at year 3 suggesting that liver disease greatly reduces life expectancy. Benhammou et al. [83] evaluated the TGR in NAFLD related HCC and viral-HCC. NAFLD-HCC was slower growing compared with other types, the TGR being highest in the case of HBV (9.4%), followed by HCV (4.9%), and NAFLD (3.6%). Factors that remained significant and independent forecaster of TGR were raised AFP levels, low albumin, and small tumor size. Today's outcomes suggest that TGR can be implemented as the basis for differentiating the treatment of HCC by etiology.

D. PRECLINICAL MODELS FOR UNDERSTANDING TUMOUR BIOLOGY

PDX for paediatric liver cancers, including HB and HCC were developed by Nicolle et al. [84]. Overall, histological and genetic analyses of the PDX models demonstrated that the models captured the histological taxonomy and mutational profiles of the primary tumours. AFP detection in blood was employed in validation, in order to confirm homogeneity between PDX and donor tumours. Collectively, this work emphasizes the value of PDX models in elucidating the pathobiology of tumours and evaluating the effects of therapies in paediatric liver cancers.

E. SURGICAL TREATMENT STRATEGIES AND THEIR IMPLICATIONS

Oliveira et al. [85] described in detail the available surgical approaches for the treatment of CRCLMs such as ALPPS and radical two-stage versus parenchymal-sparing one-stage operations. These results revealed overall survival nearly identical to each other; thus, pointing out that tumour biology and patient related factors are more influential on prognosis than surgical procedures.

Cillo et al. [86] compared ALPPS with one-stage resections in CRLM patients and noted that this concept needs to be tailored for patients. The study also pointed out several interesting findings that working on tumour biology or patient related factors makes a much bigger difference to survival compared to the procedure used.

F. PROGNOSTIC MODELS AND SURVIVAL PREDICTION

The radiomics model to predict HGP in patients with CRLM by Han et al. [87] used MRI and the 195 lesions included the training group, internal validation group and external validation group. On the contrary, the publicly proposed model used in this article provided the AUC of 0.971, 0.909, and 0.905 respectively; thus strengthening the site of radiomics for secure unelusive signals directing towards correct management of CRLM. Abdel-Wahab et al. [88] confirmed the usability and reliability of the IGF-CTP scoring system for evaluation of hepatic reserve in Egyptian population with HCC. The continued correlation analysis confirmed the IGF-CTP score's prognostic role in hepatic function and overall survival. The findings provide the basis for the routine application of this tool to address HCC-related issues and improve treatment plans.

Zhang et al. [56] provided an assessment of the role of radiomics in determining postoperative survival of patients with primary liver cancer including HCC, MCC, HCC-CHCC among others. For OS analyses, clinicopathological and radiomics features from DWI and EP images were independently associated with OS, and nomograms were developed based on these characteristics.

To understand the function of SIRT1 and c-Myc in promoting liver tumour cell survival in HCC. SIRT1 and c-Myc trans regulate each other, therefore augmenting

tumour progression. SIRT1 was significantly associated with Ki67 and p53, two well-known markers of poor prognosis and was identified as an independent predictor of HCC survival, providing a rationale for molecular targeting.

Martínez-Blanco et al. [100] proposed a machine learning-based approach to predict mortality risk at the time of HCC diagnosis by leveraging clinical and analytical data. The study employed a retrospective multicenter dataset of 191 HCC patients and utilized various machine learning models to identify key prognostic factors influencing patient outcomes. Among the models evaluated, the RF algorithm demonstrated superior performance, achieving an accuracy of 96%, a precision of 94%, a recall of 95%, an F1-score of 94%, and an AUC-ROC of 0.96. Key prognostic variables identified in the study included the Milan criteria, BCLC staging, and serum albumin levels, which were determined to have a significant impact on patient prognosis. The study highlights the importance of integrating machine learning-based predictive models into clinical workflows to assist healthcare professionals in making informed treatment decisions. The authors emphasized the potential of AI-driven models to improve personalized treatment planning and optimize resource allocation in HCC management. Despite the promising results, the study acknowledges certain limitations, including the relatively small sample size and the need for external validation across diverse populations to enhance the model's generalizability. Further studies are recommended to incorporate additional prognostic biomarkers and refine the model's predictive capabilities to ensure clinical applicability.

X. EXPLAINABILITY TECHNIQUES IN LIVER CANCER AI MODELS

XAI is increasingly important in medical applications to ensure that AI models for liver cancer are transparent and trustworthy. Recent research has explored various XAI methods—such as Grad-CAM, LIME, SHAP, and others—applied to liver tumor segmentation, classification, and prognosis. However, while these methods are widely used, their quantitative validation and clinical utility remain limited, and most findings are not yet supported by prospective studies or interpretability benchmarks.

A. XAI FOR LIVER TUMOR SEGMENTATION

XAI techniques to liver tumor segmentation models is increasingly important for building clinician trust and validating model behavior. Thaya et al. [107] integrated Grad-CAM into a deep learning segmentation framework for liver tumors, enabling visual heatmaps that highlight spatial regions influencing the model's predictions. The system achieved high segmentation performance (reported Dice score of 99%), and the Grad-CAM outputs were used to visually confirm whether the network's focus aligned with tumor boundaries. The authors noted that these explanations helped radiologists understand why certain regions were

marked as tumorous, facilitating greater acceptance of the AI model.

While such integration of Grad-CAM is often seen as a step toward interpretability, its practical utility in clinical segmentation tasks remains mixed. In many cases, Grad-CAM produces coarse and non-specific activations, especially when dealing with small or ill-defined liver lesions. This can lead to visual overlap with tumor-adjacent tissues or background liver parenchyma, which may not be clinically relevant. Few studies report numerical overlap (e.g., IoU or Dice) between Grad-CAM maps and expert-annotated tumor regions, making it difficult to assess clinical alignment. The reliance on visual plausibility without quantitative validation limits the interpretive reliability of these tools.

Additionally, Grad-CAM's dependence on gradients from final convolutional layers can reduce localization precision, especially in deeper or hybrid architectures. This is particularly problematic in liver CT or MRI where lesion contrast varies across imaging phases. Grad-CAM offers visual interpretability but at the cost of spatial accuracy—particularly in 3D volumetric settings. While the resulting heatmaps may appear intuitive, they may not reflect the true decision boundaries used by the model.

Studies like Vries et al. [103] have explored enhancements such as Guided Grad-CAM to improve spatial resolution, yet even these hybrid methods remain largely qualitative. Most literature presents XAI overlays as static visuals with limited downstream evaluation, and rarely incorporates them into real-time clinical workflows. As a result, their role in supporting clinical reasoning remains constrained unless paired with rigorous interpretability validation and quantifiable performance metrics.

To improve validation, future studies should quantify the overlap between Grad-CAM heatmaps and expert-annotated tumor masks using spatial metrics like Dice or IoU, and evaluate whether such visualizations improve radiologists' segmentation confidence.

B. XAI FOR LIVER TUMOR CLASSIFICATION AND DIAGNOSIS

XAI techniques have gained prominence in the classification of liver tumors, where model transparency is essential for clinical deployment. Whether applied to radiological imaging or histopathology, these tools aim to reveal the internal decision-making processes of AI systems, allowing clinicians to verify whether the model is focusing on medically relevant features.

In radiology, a notable example is the work by Wang et al. [102], where a CNN was developed to classify liver lesions on MRI into categories such as HCC, metastasis, and benign lesions. The system not only outperformed radiologists in sensitivity and specificity but also delivered multi-modal interpretability. Each prediction was accompanied by visual heatmaps highlighting relevant lesion features (e.g., tumor margins, enhancement zones) and textual explanations describing the model's rationale based on radiologic criteria.

These explanations appeared to align with known features, but no user study quantified whether they improved diagnostic confidence or accuracy—limiting claims of real-world impact.

Although the system showed promise, the explanations were generated post hoc and may not faithfully reflect the AI's internal reasoning. Without clinical validation—such as reader studies or interpretability scoring—it remains unclear whether these explanations aid or simply reassure clinicians. Furthermore, while CNNs can be partially explained with Grad-CAM, more complex transformer-based models may trade interpretability for performance, posing challenges for transparent decision support.

In digital pathology, similar concerns arise. Deep learning models can accurately classify liver tumors in WSIs, but their lack of interpretability hinders adoption. Grignaffini et al. [105] emphasized the need for overlay-based explanations on pathology slides to show which cellular structures influenced predictions. Grad-CAM has been used to visualize attention on histological features like trabecular patterns or stroma. However, these saliency maps lack spatial precision, and no standard metric currently assesses their validity in high-resolution histopathological tasks.

XAI methods like Grad-CAM (visual), SHAP (feature attribution), and LIME (local surrogate modeling) are increasingly used to enhance transparency. Yet, most studies stop at visual inspection without quantifying the clinical usefulness of these explanations. Their impact on diagnostic trust, accuracy, or decision-making remains largely untested in real-world settings.

Despite growing adoption, most diagnostic XAI methods are rarely tested through clinician-in-the-loop or prospective reader studies. To establish real-world value, future work should assess whether explanations measurably improve diagnostic accuracy or reduce inter-observer variability.

C. XAI FOR PROGNOSIS AND OUTCOME PREDICTION IN LIVER CANCER

Beyond diagnostic classification, AI models are increasingly used for prognosis tasks in liver cancer—such as predicting recurrence, survival, or treatment response. For these models to be actionable in clinics, their predictions must be explainable. Physicians need to understand not just the risk score, but the contributing clinical factors for each patient.

Recent work has incorporated SHAP and LIME to explain risk scores generated by models like logistic regression, SVM, random forests, and XGBoost. Guo et al. [106], for example, used SHAP to interpret an XGBoost model predicting early tumor recurrence post-ablation. Features such as tumor number, AFP levels, and platelet count were consistently ranked as high-impact predictors. This provided clinicians with interpretable outputs—e.g., “multiple tumors and high AFP suggest increased recurrence risk.”

A related study extended this by including both imaging and clinical features in a prognostic model, again using SHAP to identify influential variables. While some were expected

TABLE 7. Comparison of common XAI techniques used in liver cancer models.

XAI Method	Best Suited For	Strengths	Limitations
Grad-CAM	CNN-based models for 2D/3D imaging (CT, MRI, histopathology)	Provides intuitive visual explanations via saliency maps; easy to overlay on medical images	Coarse localization; lacks spatial precision for small or subtle lesions; no quantitative trust measure
SHAP	Tabular models (e.g., prognosis, recurrence risk prediction)	Quantifies global and local feature importance; consistent with game theory	Computationally expensive; assumes feature independence; can mislead without causal validation
LIME	Tabular or classification models with structured input	Model-agnostic; explains individual predictions using local surrogate models	Sensitive to perturbation method; unstable explanations; hard to scale to large input dimensions
Guided Grad-CAM	Image-based models (enhanced Grad-CAM)	Higher-resolution saliency; better visual focus on fine details	More complex to implement; still lacks formal alignment with annotated labels
Hybrid Approaches (e.g., SHAP + Grad-CAM)	Multimodal tasks combining imaging and clinical data	Offers both spatial and feature-level insights; improved interpretability	Higher complexity; longer runtime; limited support in off-the-shelf tools

(e.g., tumor size), others—like low potassium or higher BMI—were less intuitive, underscoring the importance of careful clinical interpretation. However, such SHAP outputs indicate statistical association, not causality, and may mislead if overinterpreted.

These models also come with a tradeoff: simpler models like XGBoost are easier to explain, while deep learning models may be more accurate but less transparent. In practice, SHAP and LIME explanations rarely undergo clinician validation or formal evaluation of interpretive utility. Most studies are retrospective, and few quantify how often the identified features align with clinical reasoning or change treatment decisions.

Although SHAP helps highlight predictive features, its real-world utility should be supported through metrics like concordance index (C-index) and decision-curve analysis to assess clinical benefit.

D. COMPARING DIFFERENT XAI TECHNIQUES IN LIVER CANCER MODELS

Several studies have compared multiple XAI techniques to evaluate their relative interpretive value in liver cancer AI applications. Grad-CAM is often favored for CNN-based imaging models due to its intuitive saliency maps, whereas SHAP and LIME are better suited to models handling tabular clinical or outcome data.

Song et al. [104] proposed a novel XAI framework, the “Explainer,” for ultrasound-based liver tumor classification, and compared it directly to Grad-CAM. In a physician reader study, the Explainer provided more clinically meaningful heatmaps and improved diagnostic accuracy. However, this was a single-center study, and its generalizability remains uncertain without replication in larger, more diverse cohorts.

Similarly, Vries et al. [103] combined multiple visual XAI techniques (Grad-CAM, Guided Backpropagation, Layer-wise Relevance Propagation) to analyze MRI-based tumor classification. They found that hybrid methods like Guided Grad-CAM yielded more precise visual attributions. In a separate skin lesion study, Vries et al. found that LIME offered more comprehensible local explanations than SHAP

or Grad-CAM variants, although these results may not directly transfer to liver imaging.

These comparisons highlight that the optimal XAI method depends on the task and data type. A comparative summary of commonly used XAI techniques in liver cancer AI models is presented in Table 7, outlining their strengths, weaknesses, and preferred application domains. Grad-CAM variants excel at showing spatial focus in image-based models, while SHAP/LIME clarify which features contribute to a prediction. Still, combining both spatial and feature explanations may provide the most comprehensive insight—though at the cost of increased computational complexity and interpretive burden.

1) NOTE ON PRACTICAL VARIABILITY

Despite their potential, XAI methods must be evaluated for consistency and reliability. Variations in scanner hardware, histological staining, and imaging protocols can influence both model predictions and the resulting explanations. Additionally, the same image may yield different saliency maps under minor model changes or input perturbations, raising concerns about explanation stability. For XAI to become clinically actionable, it must move beyond intuitive overlays and be validated through prospective trials, user studies, and quantifiable interpretability benchmarks.

XI. ROLE OF ANNOTATION TOOLS IN LIVER TUMOUR SEGMENTATION AND ANALYSIS

In medical image analysis, accurate annotation is essential for training and validating machine learning models, especially for the segmentation of liver tumours. Various annotation tools have been developed to facilitate this process, ranging from manual to semi-automatic and AI-assisted systems. These tools help in delineating liver structures, tumours, and other regions of interest, improving diagnostic accuracy and enhancing the effectiveness of AI models for liver tumour detection and segmentation.

Several tools have been widely adopted for annotating liver tumours in imaging modalities such as CT, MRI, and ultrasound. Table 8. contains some of the key annotation tools used.

TABLE 8. Medical imaging annotation tools.

Tool/Software	Key Features	Supported Modalities	License	Platform
3D Slicer [89]	Open-source, customizable, supports 3D segmentation, volumetric rendering, and Python scripting	CT, MRI, PET, ultrasound, microscopy	Open-source (BSD)	Windows, Mac, Linux
ITK-SNAP [90]	Easy-to-use, semi-automatic segmentation, supports 3D imaging	CT, MRI, ultrasound	Open-source (GPL)	Windows, Mac, Linux
Labelbox	AI-assisted labeling, collaboration features, handles large datasets	CT, MRI, X-ray	Proprietary	Web-based
MIPAV (Medical Image Processing, Analysis, and Visualization)	Advanced image processing, supports 2D/3D image visualization, and analysis	CT, MRI, PET, ultrasound	Open-source	Windows, Mac, Linux
NVIDIA Clara	AI-assisted annotation, powerful automation features, 3D and multi-modality support	CT, MRI, X-ray, ultrasound, pathology	Proprietary	Cloud-based
Apeer (Zeiss)	Focused on microscopy, integrated AI tools, user-friendly interface	Microscopy, pathology	Proprietary	Web-based
CVAT	Supports video and image annotations, strong AI integration, collaborative tools	X-ray, CT, MRI, endoscopy	Open-source (MIT)	Web-based
MedSeg	AI-based segmentation, fast annotation for common medical imaging tasks, integrates with DICOM viewer	CT, MRI, X-ray	Open-source (GPL)	Web-based
DeepLabel	Advanced AI-assisted annotations, integrates deep learning models	MRI, CT, X-ray	Proprietary	Web-based
VGG Image Annotator (VIA) [91]	Lightweight, manual image annotation tool with polygon, bounding box, and point annotations	Histopathology, radiology	Open-source (MIT)	Web-based

XII. RESEARCH CHALLENGES

One of the major challenges that currently mark AI research for liver tumour segmentation and classification is variability of image data. Current datasets like LiTS and MICCAI contain data from limited populations, which can reduce generality in patients of other demographics, different types of scanners, and varied image acquisitions. Intra-institutional variations in image quality and annotation further complicate the model-building process. Expanding existing datasets and creating new, complex, and diverse datasets containing images from multiple sites and imaging systems is necessary to develop AI algorithms that function optimally across a range of clinical scenarios.

Over-fitting remains a significant challenge, as models trained on limited datasets tend to perform well in controlled environments but fail to generalize to new clinical scenarios. Techniques such as data augmentation, transfer learning, and domain adaptation can help mitigate over-fitting and improve model robustness. Additionally, tumor morphology variability poses a challenge as tumours can present with different shapes, sizes, and textures, making it difficult for AI models to learn generalizable features. Leveraging diverse datasets and incorporating shape-aware loss functions can enhance the model's ability to handle such variability.

Another significant challenge is the limited availability of vessel segmentation studies, as hepatic vessel segmentation remains a challenge due to the scarcity of annotated datasets [94]. Additionally, most studies focus on pre-operative images, leaving a gap in tracking liver regeneration and post-surgical changes, which affects AI model generalizability [94]. The challenge of simultaneous segmentation of tumours, liver tissues, and surrounding organs persists due to low contrast and partial volume effects [94]. Furthermore, the presence of noise, imaging artifacts, and variations in contrast agent uptake across different imaging protocols make accurate segmentation

more challenging, requiring advanced noise suppression and domain adaptation techniques [94].

The combination of multiple forms of data within research also presents a challenge. Most existing work analyzes imaging datasets with a single modality, primarily CT or MRI, which limits comprehensive analysis. Integrating data from multiple modalities such as CT, MRI, pathological examination, and genomic analysis can enhance diagnostic confidence and accuracy, improve prognosis estimation, and assist in treatment planning. However, efficient approaches for combining and analyzing such diverse data are still lacking. Multimodal data fusion faces challenges due to differing spatial resolutions, noise levels, and data heterogeneity. Techniques such as attention-based fusion networks and feature selection strategies can help address these issues. Additionally, sparse and noisy genomic data introduce further difficulties, necessitating the use of imputation techniques and robust feature extraction methodologies to enhance prediction accuracy.

The explainability of AI models is another key challenge in liver tumor analysis. Many deep learning models function as “black boxes,” where their decision-making processes remain obscure to users. This lack of interpretability reduces clinician confidence in AI-assisted diagnosis and limits their adoption in clinical practice. Developing XAI techniques that present model decisions in a transparent manner can bridge the gap between research and practical healthcare applications. Methods such as attention mechanisms, feature attribution mapping, and layer-wise relevance propagation could enhance the interpretability of liver segmentation models. Furthermore, the explainability of AI models emerges as a critical challenge in liver tumor analysis, where many deep learning models function as “black boxes” and their decision-making processes remain opaque to users. This lack of interpretability not only reduces clinician confidence in AI-assisted diagnosis but also limits adoption in clinical

practice. Addressing this issue requires the development of advanced XAI techniques—such as the implementation of standardized evaluation methods for explanations, ensuring data quality to reduce bias, and tackling technical limitations like the choice of CNN layers for generating Grad-CAM—that provide transparent and reliable model decisions. Experts recommend the integration of XAI methods like SHAP and LIME to offer both global and local interpretability, alongside user-friendly interfaces and decision support tools (e.g., adjustable thresholds for visualizing segmented tumor regions or dashboards highlighting influential clinical factors). Adopting multi-center, diverse training data and fostering a culture of interpretability through regulatory and clinical mandates are also essential for bridging the gap between research and practical healthcare applications.

Moreover, high computational requirements of state-of-the-art models limit their deployment in resource-constrained clinical environments. Optimizing models to balance accuracy and computational efficiency, utilizing model compression techniques such as quantization and pruning, and exploring edge AI solutions could facilitate broader clinical adoption. Real-world deployment of AI models presents additional challenges such as integration with hospital workflows, ensuring interoperability with PACS and EHR systems, and addressing latency issues to provide real-time assistance. Further research is needed to optimize AI models for efficient clinical deployment without compromising accuracy. Multi-center validation is also crucial. Although many current models achieve high accuracy in controlled experimental conditions, they often lack validation in prospective studies across different clinical environments. Adopting diverse, multi-institutional training data and performing rigorous external validation can ensure model reliability and adaptability to various clinical workflows.

Additionally, prognostic biomarker identification using AI and radiomics remains an underexplored area. While potential biomarkers such as microvascular invasion (MVI) and tumor growth rates have shown promise, their clinical validation is still limited. Further studies are required to establish reliable imaging characteristics as predictors of clinical outcomes such as survival and recurrence, facilitating their integration into routine clinical practice.

Multi-task learning models aimed at solving segmentation, classification, and localization simultaneously present another challenge. Although significant progress has been made in developing such models, achieving consistent performance across all tasks remains difficult. The optimization of conflicting objectives and verifying model robustness in diverse clinical scenarios require further research. Addressing failure cases, such as poor imaging quality, occluded tumor boundaries, and rare pathological cases, is crucial to improving AI model reliability. Implementing uncertainty estimation techniques and active learning frameworks can help AI models better identify challenging cases and avoid erroneous predictions.

Finally, external validation of AI models in real-world clinical settings remains a significant gap. Many current models achieve high accuracy in controlled experimental conditions but lack validation in prospective studies across different clinical environments. Ensuring model reliability and adaptability to various clinical workflows is crucial for their successful deployment in healthcare settings. Furthermore, there is a need to develop and integrate methods for advanced domain adaptation to address the heterogeneity across imaging protocols, and to establish standardized benchmarks that assess model performance in diverse, multi-center datasets. However, an often-overlooked challenge lies in tailoring AI architectures to specific clinical needs. For instance, large 3D U-Net or Transformer-based models may be more suitable for complex, multi-institutional datasets and volumetric tumor segmentation, but can be computationally prohibitive in lower-resource settings. In contrast, lightweight CNNs (e.g., MobileNet) or UNet-lite variants can offer faster inference but might struggle with highly heterogeneous lesions or multi-modal inputs. Furthermore, metastases, rare subtypes, and borderline lesions may each require specialized data augmentation or domain adaptation strategies. Consequently, the choice of architecture, loss function, and even hyperparameters should align with the imaging modality, tumor type, and clinical context. Ensemble or multi-modal approaches can further improve performance—particularly when combining imaging data with pathological or genomic information—though at the cost of higher model complexity and training overhead. Ultimately, model selection hinges on striking a balance between accuracy, computational feasibility, interpretability, and the specific demands of each clinical use case.

Addressing these challenges will contribute to enhancing model accuracy, clinical applicability, and robustness across diverse patient demographics and imaging protocols.

XIII. DISCUSSION

This review comprehensively analyzes the advancements in liver tumor diagnosis and treatment, particularly emphasizing the transformative role of artificial intelligence in this domain. The literature demonstrates that AI-driven approaches, notably deep learning models such as U-Net variants, CNNs, and Transformer-based architectures, have significantly enhanced the segmentation, classification, and prognostication of liver tumors. These improvements have led to more precise diagnostic processes and personalized treatment planning. Quantitative performance metrics, including Dice coefficients and AUC values, consistently demonstrate robust performance across studies, with hybrid models and ensemble techniques often outperforming single-model approaches by effectively balancing segmentation precision and computational efficiency.

A critical aspect of clinical translation is the interpretability of these AI models. Several studies have incorporated explainable AI methods, such as class activation maps,

to elucidate which features drive model decisions. However, there remains an opportunity to broaden the discussion by integrating additional techniques like Grad-CAM, LIME, and SHAP to provide a more comprehensive understanding of the models' decision-making processes. Enhanced transparency is essential for building clinical trust and for mitigating biases that may arise from variations in staining protocols or imaging conditions.

Generalizability is another key concern that this review addresses. While some studies have reported external validation using multi-center datasets such as TCGA-LIHC, the discussion often lacks a thorough examination of cross-institutional performance. Differences in sample preparation, imaging modalities, and patient demographics can lead to significant variability in model performance. It is therefore imperative that future work emphasizes comprehensive external validation using independent cohorts from diverse institutions. This approach will ensure that the models are robust and applicable to real-world clinical settings, rather than being overfitted to a single data source.

The review also provides practical guidance for clinical model selection by comparing different architectures in the context of specific diagnostic challenges. For instance, models optimized for early-stage HCC may differ in their requirements and performance from those designed to detect metastatic tumors or rare subtypes. By examining quantitative benchmarks and evaluating computational trade-offs, this discussion helps inform decisions on which models may be most suitable for various clinical scenarios. Such clarity is essential for translating high-performance AI models into reliable tools for patient care.

Despite these promising advancements, challenges remain. Many studies are limited by single-center datasets or insufficient external validations, which raises concerns about overfitting and reduced generalizability. Variability in imaging protocols and annotation methods further complicates the translation of these technologies into clinical practice. Recognizing these limitations is crucial, and future research must focus on standardizing datasets, enhancing validation frameworks, and integrating multimodal data to address these issues.

Looking ahead, future research should concentrate on expanding multi-center and cross-institutional validations to better assess model robustness, as well as on integrating advanced explainability techniques to provide clearer insights into model decisions. Additionally, exploring multimodal integration strategies that combine imaging, clinical, and genetic data could further enhance diagnostic accuracy and personalized treatment planning. By addressing these challenges and focusing on comprehensive external validation and interpretability, the field can advance toward developing AI systems that are not only high-performing in controlled environments but also reliable and generalizable in real-world clinical applications.

XIV. CONCLUSION

In this review, recent developments on utilization of artificial intelligence for diagnosing, segmenting, and predicting liver tumour outcomes have been highlighted. They span across a wide range of methodological approaches, from the more conventional machine learning to the more state-of-the-art deep learning based approaches, with the main focus on the medical application of liver tumour image and pathology. Despite the massive advancement in diagnostic accuracy, segmentation precision, and the prognostic model, several issues must be resolved as follows. These are the growing demands for samples that contain diverse patients for generalization, better starting-point interpretability to garner better clinician adoption, and incorporating more comprehensive than unimodal data sources for whole-patient assessment. Furthermore, although multi-task learning and radiomics have been applied to prediction models, there is a significantly limited number of studies and thus stronger validation and further expansion is necessary for the applicability of these technologies in routine clinical practice. The future research should adhere to the creation of explainable AI models, use mixed data modalities, to compare the effectiveness of models in the populations of various compositions, and to search for new prognostic biomarkers for enhanced treatment individualization. Therefore, filling these gaps will not only enhance model performance, as demonstrated in our study, but also increase the level of confidence in clinicians resulting in faster penetration of AI in the treatment of liver cancer and better outcomes for patients.

ACKNOWLEDGMENT

(*Yana Gaur and Abhay Chaudhary contributed equally to this work.*)

REFERENCES

- [1] M. Xiong, Y. Xu, Y. Zhao, S. He, Q. Zhu, Y. Wu, X. Hu, and L. Liu, "Quantitative analysis of artificial intelligence on liver cancer: A bibliometric analysis," *Frontiers Oncol.*, vol. 13, Feb. 2023, Art. no. 990306.
- [2] A. T. Ciner, K. Jones, R. J. Muschel, and P. Brodt, "The unique immune microenvironment of liver metastases: Challenges and opportunities," *Seminars Cancer Biol.*, vol. 71, pp. 143–156, Jun. 2021.
- [3] J. Y. Kim, S.-M. Hong, and J. Y. Ro, "Recent updates on grading and classification of neuroendocrine tumors," *Ann. Diagnostic Pathol.*, vol. 29, pp. 11–16, Aug. 2017.
- [4] A. Magnussen, "Aflatoxins, hepatocellular carcinoma and public health," *World J. Gastroenterol.*, vol. 19, no. 10, pp. 1508–1512, Mar. 2013, doi: [10.3748/wjg.v19.i10.1508](https://doi.org/10.3748/wjg.v19.i10.1508).
- [5] C. A. Linsell and F. G. Peers, "Aflatoxin and liver cell cancer," *Trans. Roy. Soc. Tropical Med. Hygiene*, vol. 71, no. 6, pp. 471–473, Jan. 1977, doi: [10.1016/0035-9203\(77\)90136-5](https://doi.org/10.1016/0035-9203(77)90136-5).
- [6] G. N. Wogan, "Aflatoxin as a human carcinogen," *Hepatology*, vol. 30, no. 2, pp. 573–575, Aug. 1999, doi: [10.1002/hep.510300231](https://doi.org/10.1002/hep.510300231).
- [7] J. Vana, G. P. Murphy, B. L. Aronoff, and H. W. Baker, "Survey of primary liver tumors and oral contraceptive use," *J. Toxicol. Environ. Health.*, vol. 5, nos. 2–3, pp. 255–273, Mar. 1979, doi: [10.1080/15287397909529748](https://doi.org/10.1080/15287397909529748).
- [8] B. L. Warren and G. D. Bellward, "Benign liver tumors and oral contraceptive therapy," *Drug Intell. Clin. Pharmacy*, vol. 13, no. 11, pp. 680–689, Nov. 1979, doi: [10.1177/106002807901301107](https://doi.org/10.1177/106002807901301107).
- [9] S. R. Ande, K. H. Nguyen, B. L. Grégoire Nyomba, and S. Mishra, "Prohibitin-induced, obesity-associated insulin resistance and accompanying low-grade inflammation causes Nash and HCC," *Sci. Rep.*, vol. 6, no. 1, pp. 1–12, Mar. 2016, doi: [10.1038/srep23608](https://doi.org/10.1038/srep23608).

- [10] S. Waly Raphael, Z. Yangde, and C. YuXiang, "Hepatocellular carcinoma: Focus on different aspects of management," *ISRN Oncol.*, vol. 2012, pp. 1–12, May 2012, doi: [10.5402/2012/421673](https://doi.org/10.5402/2012/421673).
- [11] R. J. Felizardo, "Hepatocellular carcinoma and food contamination: Ochratoxin as a great prompter," *World J. Gastroenterol.*, vol. 19, no. 24, pp. 3723–3725, Jun. 2013, doi: [10.3748/wjg.v19.i24.3723](https://doi.org/10.3748/wjg.v19.i24.3723).
- [12] B. Sripath and C. Pairojkul, "Cholangiocarcinoma: Lessons from Thailand," *Current Opinion Gastroenterol.*, vol. 24, no. 3, pp. 349–356, May 2008, doi: [10.1097/mog.0b013e3282fbf9b3](https://doi.org/10.1097/mog.0b013e3282fbf9b3).
- [13] F. A. Baker, A.-R. Zeina, S. A. Mouch, and A. Mari, "Benign hepatic tumors: From incidental imaging finding to clinical management," *Korean J. Family Med.*, vol. 42, no. 1, pp. 2–8, Jan. 2021, doi: [10.4082/kjfm.18.0188](https://doi.org/10.4082/kjfm.18.0188).
- [14] L. C. Bertot, G. P. Jeffrey, M. Wallace, G. MacQuillan, G. Garas, H. L. Ching, and L. A. Adams, "Nonalcoholic fatty liver disease-related cirrhosis is commonly unrecognized and associated with hepatocellular carcinoma," *Hepatol. Commun.*, vol. 1, no. 1, pp. 53–60, Feb. 2017, doi: [10.1002/hep4.1018](https://doi.org/10.1002/hep4.1018).
- [15] R. W. Parks and G. C. Oniscu, "Benign conditions of the liver," *Surgery*, vol. 25, no. 1, pp. 22–27, Jan. 2007, doi: [10.1016/j.mpsur.2006.11.003](https://doi.org/10.1016/j.mpsur.2006.11.003).
- [16] H. S. Hoffman, "Benign hepatoma: Review of the literature and report of a case," *Ann. Internal Med.*, vol. 17, no. 1, pp. 130–139, Jul. 1942, doi: [10.7326/0003-4819-17-1-130](https://doi.org/10.7326/0003-4819-17-1-130).
- [17] P. R. Ros and K. C. P. Li, "Part II: Benign liver tumors," *Current Problems Diagnostic Radiol.*, vol. 18, no. 3, pp. 125–155, May 1989, doi: [10.1016/0363-0188\(89\)90027-3](https://doi.org/10.1016/0363-0188(89)90027-3).
- [18] P. R. Ros and J. F. Rasmussen, "Part I: Malignant liver tumors," *Current Problems Diagnostic Radiol.*, vol. 18, no. 3, pp. 95–124, May 1989, doi: [10.1016/0363-0188\(89\)90026-1](https://doi.org/10.1016/0363-0188(89)90026-1).
- [19] J. H. Oh and D. W. Jun, "The latest global burden of liver cancer: A past and present threat," *Clin. Mol. Hepatol.*, vol. 29, no. 2, pp. 355–357, Apr. 2023, doi: [10.3350/cmh.2023.0070](https://doi.org/10.3350/cmh.2023.0070).
- [20] S. K. Mungamuri and V. A. Mavuduru, "Role of epigenetic alterations in aflatoxin-induced hepatocellular carcinoma," *Liver Cancer Int.*, vol. 1, no. 2, pp. 41–50, Oct. 2020, doi: [10.1002/lci2.20](https://doi.org/10.1002/lci2.20).
- [21] J. Chiu, R. Pang, R. Poon, T. Yau, J. Chiu, R. Pang, R. Poon, and T. Yau, "Systemic management of advanced hepatocellular carcinoma patients: The role of multi-targeted anti-angiogenic inhibitors," in *Hepatocellular Carcinoma-Clinical Research*. London, U.K.: IntechOpen, Mar. 2012, doi: [10.5772/27152](https://doi.org/10.5772/27152).
- [22] M. M. Berman, N. P. Libbey, and J. H. Foster, "H epa to c elu la r Ca rcin om a polygonal cell type with fibrous stroma—An atypical variant with a favorable prognosis ESULTS OF SEVERAL histopathologic s t," *Cancer*, vol. 46, pp. 1448–1455, Jan. 1980, doi: [10.1002/1097-0142\(19800915\)46:6<1448::aid-cncr2820460626>3.0.co;2-j](https://doi.org/10.1002/1097-0142(19800915)46:6<1448::aid-cncr2820460626>3.0.co;2-j).
- [23] H. Malhi and G. J. Gores, "Review article: The modern diagnosis and therapy of cholangiocarcinoma," *Alimentary Pharmacol. Therapeutics*, vol. 23, no. 9, pp. 1287–1296, May 2006, doi: [10.1111/j.1365-2036.2006.02900.x](https://doi.org/10.1111/j.1365-2036.2006.02900.x).
- [24] M.-F. Chen, "Peripheral cholangiocarcinoma (cholangiocellular carcinoma): Clinical features, diagnosis and treatment," *J. Gastroenterol. Hepatol.*, vol. 14, no. 12, pp. 1144–1149, Dec. 1999, doi: [10.1046/j.1440-1746.1999.01983.x](https://doi.org/10.1046/j.1440-1746.1999.01983.x).
- [25] E. Oneda, M. Abu Hilal, and A. Zaniboni, "Biliary tract cancer: Current medical treatment strategies," *Cancers*, vol. 12, no. 5, p. 1237, May 2020, doi: [10.3390/cancers12051237](https://doi.org/10.3390/cancers12051237).
- [26] C. H. Scudamore, S. I. Lee, E. J. Patterson, A. K. Buczkowski, L. V. July, S. W. Chung, A. R. Buckley, S. G. F. Ho, and D. A. Owen, "Radiofrequency ablation followed by resection of malignant liver tumors," *Amer. J. Surg.*, vol. 177, no. 5, pp. 411–417, May 1999, doi: [10.1016/s0002-9610\(99\)00068-9](https://doi.org/10.1016/s0002-9610(99)00068-9).
- [27] T. Hennedige and S. K. Venkatesh, "Imaging of hepatocellular carcinoma: Diagnosis, staging and treatment monitoring," *Cancer Imag.*, vol. 12, no. 3, pp. 530–547, 2012, doi: [10.1102/1470-7330.2012.0044](https://doi.org/10.1102/1470-7330.2012.0044).
- [28] A. S. Kucukkaya, T. Zeevi, N. X. Chai, R. Raju, S. P. Haider, M. Elbanan, A. Petukhova-Greenstein, M. Lin, J. Onofrey, M. Nowak, K. Cooper, E. Thomas, J. Santana, B. Gebauer, D. Mulligan, L. Staib, R. Batra, and J. Chapiro, "Predicting tumor recurrence on baseline MR imaging in patients with early-stage hepatocellular carcinoma using deep machine learning," *Sci. Rep.*, vol. 13, no. 1, pp. 1–9, May 2023, doi: [10.1038/s41598-023-34439-7](https://doi.org/10.1038/s41598-023-34439-7).
- [29] A. Younas, J. Riaz, T. Chughtai, H. Maqsood, M. Saim, S. Qazi, S. Younis, U. Ghaffar, and M. Khaliq, "Hyponatremia and its correlation with hepatic encephalopathy and severity of liver disease," *Cureus*, vol. 13, no. 2, pp. e13175–e13175, Feb. 2021, doi: [10.7759/cureus.13175](https://doi.org/10.7759/cureus.13175).
- [30] F. Farinati, M. Rinaldi, S. Gianni, and R. Naccarato, "How should patients with hepatocellular carcinoma be staged? Validation of a new prognostic system," *Cancer, Interdiscipl. Int. J. Amer. Cancer Soc.*, vol. 89, no. 11, pp. 2266–2273, 2000, doi: [https://doi.org/10.1002/1097-0142\(20001201\)89:11<2266::aid-cncr15>3.0.co;2-0](https://doi.org/10.1002/1097-0142(20001201)89:11<2266::aid-cncr15>3.0.co;2-0).
- [31] P. J. Johnson, "Non-surgical treatment of hepatocellular carcinoma," *HPB*, vol. 7, no. 1, pp. 50–55, Mar. 2005, doi: [10.1002/1365-1820\(20041002\)7:1<50::aid-hpb24076](https://doi.org/10.1002/1365-1820(20041002)7:1<50::aid-hpb24076).
- [32] G. Marín-Hargreaves, D. Azoulay, and H. Bismuth, "Hepatocellular carcinoma: Surgical indications and results," *Crit. Rev. Oncol./Hematol.*, vol. 47, no. 1, pp. 13–27, Jul. 2003, doi: [10.1016/s1040-8428\(02\)00213-5](https://doi.org/10.1016/s1040-8428(02)00213-5).
- [33] M. Tsurusaki and T. Murakami, "Surgical and locoregional therapy of HCC: TACE," *Liver Cancer*, vol. 4, no. 3, pp. 165–175, Sep. 2015, doi: [10.1159/000367739](https://doi.org/10.1159/000367739).
- [34] Q. Wang, S. Liu, F. Yang, L. Gan, X. Yang, and Y. Yang, "Magnetic alginate microspheres detected by MRI fabricated using microfluidic technique and release behavior of encapsulated dual drugs," *Int. J. Nanomed.*, vol. Volume 12, pp. 4335–4347, Jun. 2017, doi: [10.2147/ijn.s13124](https://doi.org/10.2147/ijn.s13124).
- [35] A. R. Gillams, "The use of radiofrequency in cancer," *Brit. J. Cancer*, vol. 92, no. 10, pp. 1825–1829, May 2005, doi: [10.1038/sj.bjc.6602582](https://doi.org/10.1038/sj.bjc.6602582).
- [36] F. Wang, G. Malnassy, and W. Qiu, "The epigenetic regulation of microenvironment in hepatocellular carcinoma," *Frontiers Oncol.*, vol. 11, Mar. 2021, Art. no. 653037, doi: [10.3389/fonc.2021.653037](https://doi.org/10.3389/fonc.2021.653037).
- [37] C. A. Arciero and E. R. Sigurdson, "Diagnosis and treatment of metastatic disease to the liver," *Seminars Oncol.*, vol. 35, no. 2, pp. 147–159, Apr. 2008, doi: [10.1053/j.seminoncol.2007.12.004](https://doi.org/10.1053/j.seminoncol.2007.12.004).
- [38] L. Andreana, G. Isgró, L. Marelli, N. Davies, D. Yu, S. Navalkissoor, and A. K. Burroughs, "Treatment of hepatocellular carcinoma (HCC) by intra-arterial infusion of radio-emitter compounds: Trans-arterial radio-embolisation of HCC," *Cancer Treatment Rev.*, vol. 38, no. 6, pp. 641–649, Oct. 2012, doi: [10.1016/j.ctrv.2011.11.004](https://doi.org/10.1016/j.ctrv.2011.11.004).
- [39] A. Ayman, A. H. Azza, K. Yasser, R. Kakil, F. Jonas, A. B. A. Mohammed, and M. I. Zeinab, "The role of palliative care in the management of patients with advanced hepatocellular carcinoma: A single institution experience," *J. Patient Care*, vol. 2, no. 2, pp. 1–5, 2017, doi: [10.4172/2573-4598.1000112](https://doi.org/10.4172/2573-4598.1000112).
- [40] A. Singal and S. Ravi, "Regorafenib: An evidence-based review of its potential in patients with advanced liver cancer," *Core Evidence*, pp. 81–87, Jul. 2014, doi: [10.2147/ce.s48626](https://doi.org/10.2147/ce.s48626).
- [41] C. L. Chiang, F. A. S. Lee, K. S. K. Chan, V. W. Y. Lee, K. W. H. Chiu, R. L. M. Ho, J. K. S. Fong, N. S. M. Wong, W. W. L. Yip, C. S. Y. Yeung, V. W. H. Lau, K. Man, F.-M.-S. Kong, and A. C. Y. Chan, "Survival outcome analysis of stereotactic body radiotherapy and immunotherapy (SBRT-IO) versus SBRT-alone in unresectable hepatocellular carcinoma," *Liver Cancer*, vol. 13, no. 3, pp. 273–284, Jun. 2024, doi: [10.1159/000533425](https://doi.org/10.1159/000533425).
- [42] A. Serag, A. Ion-Margineanu, H. Qureshi, R. McMillan, M.-J. S. Martin, J. Diamond, P. O'Reilly, and P. Hamilton, "Translational AI and deep learning in diagnostic pathology," *Frontiers Med.*, vol. 6, Oct. 2019, Art. no. 463767, doi: [10.3389/fmed.2019.00185](https://doi.org/10.3389/fmed.2019.00185).
- [43] R. Paudyal, A. D. Shah, O. Akin, R. K. G. Do, A. S. Konar, V. Hatzoglou, U. Mahmood, N. Lee, R. J. Wong, S. Banerjee, J. Shin, H. Veeraraghavan, and A. Shukla-Dave, "Artificial intelligence in CT and MR imaging for oncological applications," *Cancers*, vol. 15, no. 9, p. 2573, Apr. 2023, doi: [10.3390/cancers15092573](https://doi.org/10.3390/cancers15092573).
- [44] M. Dave and N. Patel, "Artificial intelligence in healthcare and education," *Brit. Dental J.*, vol. 234, no. 10, pp. 761–764, May 2023, doi: [10.1038/s41415-023-5845-2](https://doi.org/10.1038/s41415-023-5845-2).
- [45] A. Beaufrière, N. Ouzir, P. E. Zafar, A. Laurent-Bellue, M. Albuquerque, G. Lubuela, J. Grégoiry, C. Guettier, K. Mondet, J.-C. Pesquet, and V. Paradis, "Primary liver cancer classification from routine tumour biopsy using weakly supervised deep learning," *JHEP Rep.*, vol. 6, no. 3, Mar. 2024, Art. no. 101008, doi: [10.1016/j.jhepr.2024.101008](https://doi.org/10.1016/j.jhepr.2024.101008).
- [46] C. Sun, A. Xu, D. Liu, Z. Xiong, F. Zhao, and W. Ding, "Deep learning-based classification of liver cancer histopathology images using only global labels," *IEEE J. Biomed. Health Informat.*, vol. 24, no. 6, pp. 1643–1651, Jun. 2020, doi: [10.1109/JBHI.2019.2949837](https://doi.org/10.1109/JBHI.2019.2949837).
- [47] A. Kiani et al., "Impact of a deep learning assistant on the histopathologic classification of liver cancer," *NPJ Digit. Med.*, vol. 3, no. 1, pp. 1–8, Feb. 2020, doi: [10.1038/s41746-020-0232-8](https://doi.org/10.1038/s41746-020-0232-8).

- [48] Y.-S. Lin, P.-H. Huang, and Y.-Y. Chen, "Deep learning-based hepatocellular carcinoma histopathology image classification: Accuracy versus training dataset size," *IEEE Access*, vol. 9, pp. 33144–33157, 2021, doi: [10.1109/ACCESS.2021.3060765](https://doi.org/10.1109/ACCESS.2021.3060765).
- [49] M. Chen, B. Zhang, W. Topatana, J. Cao, H. Zhu, S. Juengpanich, Q. Mao, H. Yu, and X. Cai, "Classification and mutation prediction based on histopathology H&E images in liver cancer using deep learning," *NPJ Precis. Oncol.*, vol. 4, no. 1, p. 14, Jun. 2020, doi: [10.1038/s41698-020-0120-3](https://doi.org/10.1038/s41698-020-0120-3).
- [50] A. A. Aatreesh, K. Alabhyha, S. Lal, J. Kini, and P. P. Saxena, "LiverNet: Efficient and robust deep learning model for automatic diagnosis of sub-types of liver hepatocellular carcinoma cancer from H&E stained liver histopathology images," *Int. J. Comput. Assist. Radiol. Surg.*, vol. 16, no. 9, pp. 1549–1563, Sep. 2021, doi: [10.1007/s11548-021-02410-4](https://doi.org/10.1007/s11548-021-02410-4).
- [51] S. Lal, D. Das, K. Alabhyha, A. Kanfade, A. Kumar, and J. Kini, "NucleiSegNet: Robust deep learning architecture for the nuclei segmentation of liver cancer histopathology images," *Comput. Biol. Med.*, vol. 128, Jan. 2021, Art. no. 104075, doi: [10.1016/j.combiomed.2020.104075](https://doi.org/10.1016/j.combiomed.2020.104075).
- [52] S. Roy, D. Das, S. Lal, and J. Kini, "Novel edge detection method for nuclei segmentation of liver cancer histopathology images," *J. Ambient Intell. Humanized Comput.*, vol. 14, no. 1, pp. 479–496, Jan. 2023, doi: [10.1007/s12652-021-03308-4](https://doi.org/10.1007/s12652-021-03308-4).
- [53] L. Huang, H. Sun, L. Sun, K. Shi, Y. Chen, X. Ren, Y. Ge, D. Jiang, X. Liu, W. Knoll, Q. Zhang, and Y. Wang, "Rapid, label-free histopathological diagnosis of liver cancer based on Raman spectroscopy and deep learning," *Nature Commun.*, vol. 14, no. 1, pp. 1–14, Jan. 2023, doi: [10.1038/s41467-022-35696-2](https://doi.org/10.1038/s41467-022-35696-2).
- [54] Y. Feng, A. Hafiane, and H. Laurent, "A deep learning based multiscale approach to segment the areas of interest in whole slide images," *Computerized Med. Imag. Graph.*, vol. 90, Jun. 2021, Art. no. 101923, doi: [10.1016/j.compmedimag.2021.101923](https://doi.org/10.1016/j.compmedimag.2021.101923).
- [55] H. Liao, Y. Long, R. Han, W. Wang, L. Xu, M. Liao, Z. Zhang, Z. Wu, X. Shang, X. Li, J. Peng, K. Yuan, and Y. Zeng, "Deep learning-based classification and mutation prediction from histopathological images of hepatocellular carcinoma," *Clin. Transl. Med.*, vol. 10, no. 2, Jun. 2020, Art. no. e102, doi: [10.1002/ctm.2.102](https://doi.org/10.1002/ctm.2.102).
- [56] J. Zhang, X. Wang, L. Zhang, L. Yao, X. Xue, S. Zhang, X. Li, Y. Chen, P. Pang, D. Sun, J. Xu, Y. Shi, and F. Chen, "Radiomics predict postoperative survival of patients with primary liver cancer with different pathological types," *Ann. Transl. Med.*, vol. 8, no. 13, p. 820, Jul. 2020, doi: [10.21037/atm-19-4668](https://doi.org/10.21037/atm-19-4668).
- [57] L. Meng, Q. Zhang, and S. Bu, "Two-stage liver and tumor segmentation algorithm based on convolutional neural network," *Diagnostics*, vol. 11, no. 10, p. 1806, Sep. 2021, doi: [10.3390/diagnostics11101806](https://doi.org/10.3390/diagnostics11101806).
- [58] P. K. Balasubramanian, W.-C. Lai, G. H. Seng, C. Kavitha, and J. Selvaraj, "APESTNet with mask R-CNN for liver tumor segmentation and classification," *Cancers*, vol. 15, no. 2, p. 330, Jan. 2023, doi: [10.3390/cancers15020330](https://doi.org/10.3390/cancers15020330).
- [59] C.-L. Kuo, S.-C. Cheng, C.-L. Lin, K.-F. Hsiao, and S.-H. Lee, "Texture-based treatment prediction by automatic liver tumor segmentation on computed tomography," in *Proc. Int. Conf. Comput., Inf. Telecommun. Syst. (CITS)*, Jul. 2017, pp. 128–132, doi: [10.1109/CITS.2017.8035318](https://doi.org/10.1109/CITS.2017.8035318).
- [60] R. M. Ghoniem, "A novel bio-inspired deep learning approach for liver cancer diagnosis," *Information*, vol. 11, no. 2, p. 80, Jan. 2020, doi: [10.3390/info11020080](https://doi.org/10.3390/info11020080).
- [61] W. G. Negassa, S. Mishra, and H. D. Bizuneh, "Liver tumor detection and classification using GWO-ELM model," in *Proc. Int. Conf. Adv. Power, Signal, Inf. Technol. (APSIT)*, Jun. 2023, pp. 526–531, doi: [10.1109/APSIT58554.2023.10201687](https://doi.org/10.1109/APSIT58554.2023.10201687).
- [62] R. Hablani, S. Patil, and D. Kirange, "Improved salp swarm optimization-based fuzzy centroid region growing for liver tumor segmentation and deep learning oriented classification," *Int. J. Next-Gener. Comput.*, vol. 13, Nov. 2022, doi: [10.47164/ijngc.v13i5.902](https://doi.org/10.47164/ijngc.v13i5.902).
- [63] Y. Qi, W. Xiong, W. K. Leow, Q. Tian, J. Zhou, J. Liu, T. Han, S. Venkatesh, and S.-C. Wang, "Semi-automatic segmentation of liver tumors from CT scans using Bayesian rule-based 3D region growing," *MIDAS J.*, Jul. 2008, doi: [10.54294/rofibw](https://doi.org/10.54294/rofibw).
- [64] K.-B. Kim, C. W. Kim, and G. H. Kim, "Area extraction of the liver and hepatocellular carcinoma in CT scans," *J. Digit. Imag.*, vol. 21, no. S1, pp. 89–103, Oct. 2008, doi: [10.1007/s10278-007-9053-4](https://doi.org/10.1007/s10278-007-9053-4).
- [65] N. H. Abdel-massieh, M. M. Hadhoud, and K. M. Amin, "Fully automatic liver tumor segmentation from abdominal CT scans," in *Proc. Int. Conf. Comput. Eng. Syst.*, Nov. 2010, pp. 197–202, doi: [10.1109/ICCES.2010.5674853](https://doi.org/10.1109/ICCES.2010.5674853).
- [66] S. Almotairi, G. Kareem, M. Aouf, B. Almutairi, and M. A.-M. Salem, "Liver tumor segmentation in CT scans using modified SegNet," *Sensors*, vol. 20, no. 5, p. 1516, Mar. 2020, doi: [10.3390/s20051516](https://doi.org/10.3390/s20051516).
- [67] Y. Tsuchimura, S. Funabasama, J. Aoki, S. Sanada, and K. Endo, "Quantitative perfusion map of malignant liver tumors, created from dynamic computed tomography data1," *Academic Radiol.*, vol. 11, no. 2, pp. 215–223, Feb. 2004, doi: [10.1016/s1076-6332\(03\)00578-6](https://doi.org/10.1016/s1076-6332(03)00578-6).
- [68] Y. Tan and E. H. Xiao, "Rare hepatic malignant tumours: Dynamic CT, MRI, and clinicopathologic features: With analysis of 54 cases and review of the literature," *Abdom. Imag.*, vol. 38, no. 3, pp. 511–526, Jun. 2013, doi: [10.1007/s00261-012-9918-y](https://doi.org/10.1007/s00261-012-9918-y).
- [69] J. T. Ferrucci, "Liver tumor imaging," *Cancer*, vol. 67, no. S4, pp. 1189–1195, Feb. 1991, doi: [https://doi.org/10.1002/1097-0142\(19910215\)67:4<1189::AID-CNCR2820671514>3.0.CO;2-23](https://doi.org/10.1002/1097-0142(19910215)67:4<1189::AID-CNCR2820671514>3.0.CO;2-23).
- [70] A. K. Vasireddi, M. E. Leo, and J. H. Squires, "Magnetic resonance imaging of pediatric liver tumours," *Pediatric Radiol.*, vol. 52, no. 2, pp. 177–188, Feb. 2022, doi: [10.1007/s00247-021-05058-z](https://doi.org/10.1007/s00247-021-05058-z).
- [71] A. Kirilova, G. Lockwood, P. Choi, N. Bana, M. A. Haider, K. K. Brock, C. Eccles, and L. A. Dawson, "Three-dimensional motion of liver tumors using cine-magnetic resonance imaging," *Int. J. Radiat. Oncol. Biol. Phys.*, vol. 71, no. 4, pp. 1189–1195, Jul. 2008, doi: [10.1016/j.ijrobp.2007.11.026](https://doi.org/10.1016/j.ijrobp.2007.11.026).
- [72] N. Nishida and M. Kudo, "Artificial intelligence in medical imaging and its application in sonography for the management of liver tumor," *Frontiers Oncol.*, vol. 10, Dec. 2020, Art. no. 594580, doi: [10.3389/fonc.2020.594580](https://doi.org/10.3389/fonc.2020.594580).
- [73] J. H. M. Chan, E. Y. K. Tsui, S. H. Luk, A. S. L. Fung, M. K. Yuen, M. L. Szeto, Y. K. Cheung, and K. P. C. Wong, "Diffusion-weighted MR imaging of the liver: Distinguishing hepatic abscess from cystic or necrotic tumor," *Abdominal Imag.*, vol. 26, no. 2, pp. 161–165, Mar. 2001, doi: [10.1007/s002610000122](https://doi.org/10.1007/s002610000122).
- [74] M. Wagner, S. Doblas, J.-L. Daire, V. Paradis, N. Haddad, H. Leitão, P. Garteiser, V. Vilgrain, R. Sinkus, and B. E. Van Beers, "Diffusion-weighted MR imaging for the regional characterization of liver tumors," *Radiology*, vol. 264, no. 2, pp. 464–472, Aug. 2012, doi: [10.1148/radiol.12111530](https://doi.org/10.1148/radiol.12111530).
- [75] S.-H. Zhen, M. Cheng, Y.-B. Tao, Y.-F. Wang, S. Juengpanich, Z.-Y. Jiang, Y.-K. Jiang, Y.-Y. Yan, W. Lu, J.-M. Lue, J.-H. Qian, Z.-Y. Wu, J.-H. Sun, H. Lin, and X.-J. Cai, "Deep learning for accurate diagnosis of liver tumor based on magnetic resonance imaging and clinical data," *Frontiers Oncol.*, vol. 10, May 2020, Art. no. 536190, doi: [10.3389/fonc.2020.00680](https://doi.org/10.3389/fonc.2020.00680).
- [76] A. Goehler, T.-M. Harry Hsu, R. Lacson, I. Gujrathi, R. Hashemi, G. Chlebus, P. Szolovits, and R. Khorasani, "Three-dimensional neural networks to automatically assess liver tumor burden change on consecutive liver MRIs," *J. Amer. College Radiol.*, vol. 17, no. 11, pp. 1475–1484, Nov. 2020, doi: [10.1016/j.jacr.2020.06.033](https://doi.org/10.1016/j.jacr.2020.06.033).
- [77] R. S. Pinheiro, P. Herman, R. M. Lupinacci, Q. Lai, E. S. Mello, F. F. Coelho, M. V. Perini, V. Pugliese, W. Andraus, I. Ceconello, and L. C. D'Albuquerque, "Tumor growth pattern as predictor of colorectal liver metastasis recurrence," *Amer. J. Surg.*, vol. 207, no. 4, pp. 493–498, Apr. 2014, doi: [10.1016/j.amjsurg.2013.05.015](https://doi.org/10.1016/j.amjsurg.2013.05.015).
- [78] S. Wei, Y. Han, H. Zeng, S. Ye, J. Cheng, F. Chai, J. Wei, J. Zhang, N. Hong, Y. Bao, J. Zhou, Y. Ye, X. Meng, Y. Zhou, Y. Deng, M. Qiu, J. Tian, and Y. Wang, "Radiomics diagnosed histopathological growth pattern in prediction of response and 1-year progression free survival for colorectal liver metastases patients treated with bevacizumab containing chemotherapy," *Eur. J. Radiol.*, vol. 142, Sep. 2021, Art. no. 109863, doi: [10.1016/j.ejrad.2021.109863](https://doi.org/10.1016/j.ejrad.2021.109863).
- [79] J. Cheng, J. Wei, T. Tong, W. Sheng, Y. Zhang, Y. Han, D. Gu, N. Hong, Y. Ye, J. Tian, and Y. Wang, "Prediction of histopathologic growth patterns of colorectal liver metastases with a noninvasive imaging method," *Ann. Surgical Oncol.*, vol. 26, no. 13, pp. 4587–4598, Dec. 2019, doi: [10.1245/s10434-019-07910-x](https://doi.org/10.1245/s10434-019-07910-x).
- [80] E. Latacz, P.-J. van Dam, C. Vanhove, L. Llado, B. Descamps, N. Ruiz, I. Joye, D. Grünhagen, S. Van Laere, P. Dirix, D. G. Mollevi, C. Verhoeft, L. Dirix, and P. Vermeulen, "Can medical imaging identify the histopathological growth patterns of liver metastases?" *Seminars Cancer Biol.*, vol. 71, pp. 33–41, Jun. 2021, doi: [10.1016/j.semancer.2020.07.002](https://doi.org/10.1016/j.semancer.2020.07.002).

- [81] I. A. Hanouneh, C. Macaron, R. Lopez, F. Aucejo, and N. N. Zein, "Rate of tumor growth predicts recurrence of hepatocellular carcinoma after liver transplantation in patients beyond Milan or UCSF criteria," *Transplantation Proc.*, vol. 43, no. 10, pp. 3813–3818, Dec. 2011, doi: [10.1016/j.transproceed.2011.09.043](https://doi.org/10.1016/j.transproceed.2011.09.043).
- [82] L. Barbara, G. Benzi, S. Gaiani, F. Fusconi, G. Zironi, S. Siringo, A. Rigamonti, C. Barbara, W. Grigioni, A. Mazzotti, and L. Bolondi, "Natural history of small untreated hepatocellular carcinoma in cirrhosis: A multivariate analysis of prognostic factors of tumor growth rate and patient survival," *Hepatology*, vol. 16, no. 1, pp. 132–137, 1992, doi: [10.1002/hep.1840160122](https://doi.org/10.1002/hep.1840160122).
- [83] J. N. Benhammou, J. Lin, E. S. Aby, D. Markovic, S. S. Raman, D. S. Lu, and M. J. Tong, "Nonalcoholic fatty liver disease-related hepatocellular carcinoma growth rates and their clinical outcomes," *Hepatoma Res.*, vol. 7, p. 5, Nov. 2021, doi: [10.20517/2394-5079.2021.74](https://doi.org/10.20517/2394-5079.2021.74).
- [84] D. Nicolle et al., "Patient-derived mouse xenografts from pediatric liver cancer predict tumor recurrence and advise clinical management," *Hepatology*, vol. 64, no. 4, pp. 1121–1135, Oct. 2016, doi: [10.1002/hep.28621](https://doi.org/10.1002/hep.28621).
- [85] R. C. Oliveira, H. Alexandrino, M. A. Cipriano, F. C. Alves, and J. G. Tralhão, "Predicting liver metastases growth patterns: Current status and future possibilities," *Seminars Cancer Biol.*, vol. 71, pp. 42–51, Jun. 2021, doi: [10.1016/j.semcancer.2020.07.007](https://doi.org/10.1016/j.semcancer.2020.07.007).
- [86] U. Cillo, "Prediction of hepatocellular carcinoma biological behavior in patient selection for liver transplantation," *World J. Gastroenterol.*, vol. 22, no. 1, pp. 232–252, Jan. 2016, doi: [10.3748/wjg.v22.i1.232](https://doi.org/10.3748/wjg.v22.i1.232).
- [87] Y. Han, F. Chai, J. Wei, Y. Yue, J. Cheng, D. Gu, Y. Zhang, T. Tong, W. Sheng, N. Hong, Y. Ye, Y. Wang, and J. Tian, "Identification of predominant histopathological growth patterns of colorectal liver metastasis by multi-habitat and multi-sequence based radiomics analysis," *Frontiers Oncol.*, vol. 10, Aug. 2020, Art. no. 518700, doi: [10.3389/fonc.2020.01363](https://doi.org/10.3389/fonc.2020.01363).
- [88] R. Abdel-Wahab, S. Lacin, A. S. Shalaby, M. Hassan, L. Xiao, J. Morris, H. M. Amin, and A. O. Kaseb, "Impact of integrating insulin like growth factor-1 (IGF-1) in model for end stage liver disease (MELD) scores on predicting hepatocellular carcinoma patients' survival," *J. Clin. Oncol.*, vol. 34, p. 4080, May 2016, doi: [10.1200/jco.2016.34.15_suppl.4080](https://doi.org/10.1200/jco.2016.34.15_suppl.4080).
- [89] A. Fedorov, R. Beichel, J. Kalpathy-Cramer, J. Finet, J.-C. Fillion-Robin, S. Pujol, C. Bauer, D. Jennings, F. Fennessy, M. Sonka, J. Buatti, S. Aylward, J. V. Miller, S. Pieper, and R. Kikinis, "3D slicer as an image computing platform for the quantitative imaging network," *Magn. Reson. Imag.*, vol. 30, no. 9, pp. 1323–1341, Nov. 2012, doi: [10.1016/j.mri.2012.05.001](https://doi.org/10.1016/j.mri.2012.05.001).
- [90] P. A. Yushkevich, J. Piven, H. C. Hazlett, R. G. Smith, S. Ho, J. C. Gee, and G. Gerig, "User-guided 3D active contour segmentation of anatomical structures: Significantly improved efficiency and reliability," *NeuroImage*, vol. 31, no. 3, pp. 1116–1128, Jul. 2006, doi: [10.1016/j.neuroimage.2006.01.015](https://doi.org/10.1016/j.neuroimage.2006.01.015).
- [91] A. Dutta and A. Zisserman, "The VIA annotation software for images, audio and video," in *Proc. 27th ACM Int. Conf. Multimedia*, Oct. 2019, pp. 2276–2279, doi: [10.1145/3343031.3350535](https://doi.org/10.1145/3343031.3350535).
- [92] C. Tiraboschi, F. Parenti, F. Sangalli, A. Resovi, D. Belotti, and E. Lanzarone, "Automatic segmentation of metastatic livers by means of U-Net-based procedures," *Cancers*, vol. 16, no. 24, p. 4159, Dec. 2024, doi: [10.3390/cancers16244159](https://doi.org/10.3390/cancers16244159).
- [93] L. Sun, L. Jiang, M. Wang, Z. Wang, and Y. Xin, "A multi-scale liver tumor segmentation method based on residual and hybrid attention enhanced network with contextual integration," *Sensors*, vol. 24, no. 17, p. 5845, Sep. 2024, doi: [10.3390/s24175845](https://doi.org/10.3390/s24175845).
- [94] A. Al-Kababji, F. Bensaali, S. P. Dakua, and Y. Himeur, "Automated liver tissues delineation techniques: A systematic survey on machine learning current trends and future orientations," *Eng. Appl. Artif. Intell.*, vol. 117, Jan. 2023, Art. no. 105532, doi: [10.1016/j.engappai.2022.105532](https://doi.org/10.1016/j.engappai.2022.105532).
- [95] A. M. Hendi, M. A. Hossain, N. A. Majrashi, S. Limkar, B. M. Elamin, and M. Rahman, "Adaptive method for exploring deep learning techniques for subtyping and prediction of liver disease," *Appl. Sci.*, vol. 14, no. 4, p. 1488, Feb. 2024, doi: [10.3390/app14041488](https://doi.org/10.3390/app14041488).
- [96] M. A. Jumaah, Y. H. Ali, and T. A. Rashid, "Artificial liver classifier: A new alternative to conventional machine learning models," 2025, *arXiv:2501.08074*.
- [97] V.-B.-S. Zossou, F. H. R. Gnangnon, O. Biaou, F. de Vathaire, R. S. Allodji, and E. C. Ezin, "Radiomics-based classification of tumor and healthy liver on computed tomography images," *Cancers*, vol. 16, no. 6, p. 1158, Mar. 2024, doi: [10.3390/cancers16061158](https://doi.org/10.3390/cancers16061158).
- [98] T. Mocan, M. Kornek, Z. Spärchez, S. Kranjc, K. Sridhar, W. Lai, and B. Kavin, "Detection of liver tumour using deep learning based segmentation with coot extreme learning model," *Biomedicines*, vol. 11, no. 3, p. 800, Mar. 2023, doi: [10.3390/biomedicines11030800](https://doi.org/10.3390/biomedicines11030800).
- [99] V. Granata, R. Fusco, M. C. Brunese, G. Ferrara, F. Tatangelo, A. Ottaiello, A. Avallone, V. Miele, N. Normanno, F. Izzo, and A. Petrillo, "Machine learning and radiomics analysis for tumor budding prediction in colorectal liver metastases magnetic resonance imaging assessment," *Diagnostics*, vol. 14, no. 2, p. 152, Jan. 2024, doi: [10.3390/diagnostics14020152](https://doi.org/10.3390/diagnostics14020152).
- [100] P. Martínez-Blanco, M. Suárez, S. Gil-Rojas, A. M. Torres, N. Martínez-García, P. Blasco, M. Torralba, and J. Mateo, "Prognostic factors for mortality in hepatocellular carcinoma at diagnosis: Development of a predictive model using artificial intelligence," *Diagnostics*, vol. 14, no. 4, p. 406, Feb. 2024, doi: [10.3390/diagnostics14040406](https://doi.org/10.3390/diagnostics14040406).
- [101] Y. N. Gowda, R. V. Manjunath, B. Shubha, P. Prabha, N. Aishwarya, and H. M. Manu, "Deep learning technique for automatic liver and liver tumor segmentation in CT images," *J. Liver Transplant.*, vol. 17, no. 3, Dec. 2024, Art. no. 100251, Dec. 2024, doi: [10.1016/j.liver.2024.100251](https://doi.org/10.1016/j.liver.2024.100251).
- [102] C. J. Wang, C. A. Hamm, L. J. Savic, M. Ferrante, I. Schobert, T. Schlachter, M. Lin, J. C. Weinreb, J. S. Duncan, J. Chapiro, and B. Letzen, "Deep learning for liver tumor diagnosis Part II: Convolutional neural network interpretation using radiologic imaging features," *Eur. Radiol.*, vol. 29, no. 7, pp. 3348–3357, Jul. 2019, doi: [10.1007/s00330-019-06214-8](https://doi.org/10.1007/s00330-019-06214-8).
- [103] B. M. de Vries, G. J. C. Zwezerijnen, G. L. Burchell, F. H. P. van Velden, C. W. Menke-Van Der Houven Van Oordt, and R. Boellaard, "Explainable artificial intelligence (XAI) in radiology and nuclear medicine: A literature review," *Frontiers Med.*, vol. 10, May 2023, Art. no. 1180773, doi: [10.3389/fmed.2023.1180773](https://doi.org/10.3389/fmed.2023.1180773).
- [104] D. Song, J. Yao, Y. Jiang, S. Shi, C. Cui, L. Wang, L. Wang, H. Wu, H. Tian, X. Ye, D. Ou, W. Li, N. Feng, W. Pan, M. Song, J. Xu, D. Xu, L. Wu, and F. Dong, "A new xAI framework with feature explainability for tumors decision-making in ultrasound data: Comparing with grad-CAM," *Comput. Methods Programs Biomed.*, vol. 235, Jun. 2023, Art. no. 107527, doi: [10.1016/j.cmpb.2023.107527](https://doi.org/10.1016/j.cmpb.2023.107527).
- [105] F. Grignaffini, F. Barbuto, M. Troiano, L. Piazzo, P. Simeoni, F. Mangini, C. De Stefanis, A. Onetti Muda, F. Frezza, and A. Alisi, "The use of artificial intelligence in the liver histopathology field: A systematic review," *Diagnostics*, vol. 14, no. 4, p. 388, Feb. 2024, doi: [10.3390/diagnostics14040388](https://doi.org/10.3390/diagnostics14040388).
- [106] F. Guo, "Research progress on machine algorithm prediction of liver cancer prognosis after intervention therapy," *Amer. J. Cancer Res.*, vol. 14, no. 9, pp. 4580–4596, 2024, doi: [10.62347/beao1926](https://doi.org/10.62347/beao1926).
- [107] I. M. Thaya, S. Sasirekha, N. Arun, and G. Kanyalakshmi, "An XAI-driven support system to enhance the detection and diagnosis of liver tumor for interventional radiologist," *J. Inf. Syst. Eng. Manage.*, vol. 10, no. 11s, pp. 40–46, Feb. 2025, doi: [10.52783/jisem.v10i11s.1492](https://doi.org/10.52783/jisem.v10i11s.1492).
- [108] X. Li, H. Chen, X. Qi, Q. Dou, C.-W. Fu, and P.-A. Heng, "H-DenseUNet: Hybrid densely connected UNet for liver and tumor segmentation from CT volumes," *IEEE Trans. Med. Imag.*, vol. 37, no. 12, pp. 2663–2674, Dec. 2018, doi: [10.1109/TMI.2018.2845918](https://doi.org/10.1109/TMI.2018.2845918).
- [109] B. Lambert, P. Roca, F. Forbes, S. Doyle, and M. Dojat, "Anisotropic hybrid networks for liver tumor segmentation with uncertainty quantification," in *Proc. Int. Conf. Med. Image Comput. Comput.-Assist. Intervent.* (Lecture Notes in Computer Science (LNCS)), vol. 14394, Cham, Switzerland: Springer, Aug. 2023, pp. 347–356.
- [110] F. Isensee, P. F. Jaeger, S. A. A. Kohl, J. Petersen, and K. H. Maier-Hein, "NuU-net: A self-configuring method for deep learning-based biomedical image segmentation," *Nature Methods*, vol. 18, no. 2, pp. 203–211, Feb. 2021, doi: [10.1038/s41592-020-01008-z](https://doi.org/10.1038/s41592-020-01008-z).
- [111] O. Oktay, J. Schlemper, L. Le Folgoc, M. Lee, M. Heinrich, K. Misawa, K. Mori, S. McDonagh, N. Y. Hammerla, B. Kainz, B. Glocker, and D. Rueckert, "Attention U-Net: Learning where to look for the pancreas," 2018, *arXiv:1804.03999*.
- [112] J. Chen, J. Mei, X. Li, Y. Lu, Q. Yu, Q. Wei, X. Luo, Y. Xie, E. Adeli, Y. Wang, M. P. Lungren, S. Zhang, L. Xing, L. Lu, A. Yuille, and Y. Zhou, "TransUNet: Rethinking the U-Net architecture design for medical image segmentation through the lens of transformers," *Med. Image Anal.*, vol. 97, Oct. 2024, Art. no. 103280, doi: [10.1016/j.media.2024.103280](https://doi.org/10.1016/j.media.2024.103280).

- [113] A. Hatamizadeh, V. Nath, Y. Tang, D. Yang, H. R. Roth, and D. Xu, “Swin UNETR: Swin transformers for semantic segmentation of brain tumours in MRI images,” in *Proc. Int. MICCAI Brainlesion workshop*, in Lecture Notes in Computer Science, vol. 12962, 2022, pp. 272–284, doi: [10.1007/978-3-031-08999-2_22](https://doi.org/10.1007/978-3-031-08999-2_22).
- [114] M. Kang, C.-M. Ting, F. F. Ting, and C.-W. R. Phan, “Cafctnet: A CNN-transformer hybrid network with contextual and attentional feature fusion for liver tumor segmentation,” in *Proc. IEEE Int. Conf. Image Process. (ICIP)*, Oct. 2024, pp. 2970–2974, doi: [10.1109/ICIP51287.2024.10647768](https://doi.org/10.1109/ICIP51287.2024.10647768).
- [115] Z. Wang, S. Fu, S. Fu, D. Li, D. Liu, Y. Yao, H. Yin, and L. Bai, “Hybrid Gabor attention convolution and transformer interaction network with hierarchical monitoring mechanism for liver and tumor segmentation,” *Sci. Rep.*, vol. 15, no. 1, pp. 1–19, Mar. 2025, doi: [10.1038/s41598-025-90151-8](https://doi.org/10.1038/s41598-025-90151-8).
- [116] J. Shao, S. Luan, Y. Ding, X. Xue, B. Zhu, and W. Wei, “Attention connect network for liver tumor segmentation from CT and MRI images,” *Technol. Cancer Res. Treatment*, vol. 23, Jan. 2024, Art. no. 15330338231219366, doi: [10.1177/15330338231219366](https://doi.org/10.1177/15330338231219366).
- [117] W. Zhang, Y. Tao, Z. Huang, Y. Li, Y. Chen, T. Song, X. Ma, and Y. Zhang, “Multi-phase features interaction transformer network for liver tumor segmentation and microvascular invasion assessment in contrast-enhanced CT,” *Math. Biosci. Eng.*, vol. 21, no. 4, pp. 5735–5761, 2024, doi: [10.3934/mbe.20242453](https://doi.org/10.3934/mbe.20242453).
- [118] S. Chen, L. Lin, P. Cheng, Z. C. Jin, J. J. Chen, H. D. Zhu, K. K. Y. Wong, and X. Tang, “Diff4MMLITS: Advanced multimodal liver tumor segmentation via diffusion-based image synthesis and alignment,” 2024, *arXiv:2412.20418*.
- [119] A. F. Al-Battal, V. H. Tang, Q. D. Tran, S. Q. H. Truong, C. Phan, T. Q. Nguyen, and C. An, “Enhancing lesion detection in liver and kidney CT scans via lesion mask selection from two models: A main model and a model focused on small lesions,” *Comput. Biol. Med.*, vol. 186, Mar. 2025, Art. no. 109602, doi: [10.1016/j.combiomed.2024.109602](https://doi.org/10.1016/j.combiomed.2024.109602).
- [120] Z. Zhao, R. Cai, K. Xu, Z. Liu, X. Yang, J. Cheng, and C. Guan, “Multi-dataset collaborative learning for liver tumor segmentation,” in *Proc. 46th Annu. Int. Conf. IEEE Eng. Med. Biol. Soc. (EMBC)*, Jul. 2024, pp. 1–4, doi: [10.1109/EMBC53108.2024.10781844](https://doi.org/10.1109/EMBC53108.2024.10781844).
- [121] R. Shan, C. Pei, Q. Fan, J. Liu, D. Wang, S. Yang, and X. Wang, “Artificial intelligence-assisted platform performs high detection ability of hepatocellular carcinoma in CT images: An external clinical validation study,” *BMC Cancer*, vol. 25, no. 1, p. 154, Jan. 2025, doi: [10.1186/s12885-025-13529-x](https://doi.org/10.1186/s12885-025-13529-x).
- [122] J. Xie, J. Zhou, M. Yang, L. Xu, T. Li, H. Jia, Y. Gong, X. Li, B. Song, Y. Wei, and M. Liu, “Lesion segmentation method for multiple types of liver cancer based on balanced dice loss,” *Med. Phys.*, vol. 52, no. 5, pp. 3059–3074, May 2025, doi: [10.1002/mp.17624](https://doi.org/10.1002/mp.17624).
- [123] M. Yang, Z. Wu, H. Zheng, L. Huang, W. Ding, L. Pan, and L. Yin, “Cross-modality medical image segmentation via enhanced feature alignment and cross pseudo supervision learning,” *Diagnostics*, vol. 14, no. 16, p. 1751, Aug. 2024, doi: [10.3390/diagnostics14161751](https://doi.org/10.3390/diagnostics14161751).



YANA GAUR is currently pursuing the B.Tech. degree in computer science and engineering with Bennett University, specializing in data science and artificial intelligence.

She has authored several research articles and holds multiple patents in healthcare technology, showcasing her dedication to leveraging AI for impactful societal advancements. Her patents focus on innovative health monitoring systems, healthcare support frameworks, and predictive modeling for biomedical applications, emphasizing her commitment to AI-driven solutions in health and wellness. Her research spans diverse areas, including clinical decision support, diagnostics, and sports performance analytics, with publications in respected venues, such as IEEE, Springer, and Elsevier. Her interdisciplinary work highlights her commitment to advancing technology for health optimization, aiming to drive meaningful, and data-driven solutions in healthcare and beyond.



ABHAY CHAUDHARY is currently pursuing the B.Tech. degree in computer science and engineering with Bennett University, where he focuses on data science and artificial intelligence.

He is an Active Researcher. He has co-authored numerous research articles and holds multiple patents in healthcare technology. His patented inventions span innovative health monitoring systems, healthcare support mechanisms, and predictive models for biomedical applications, showcasing his commitment to pioneering technology-driven healthcare solutions. His research interests include advanced clinical decision support, diagnostic frameworks, and the application of AI in sports performance analysis. He has presented his work in top-tier conferences and journals, including IEEE, Springer, and Elsevier, reflecting his dedication to developing AI-powered solutions with real-world impact. His work emphasizes the role of interdisciplinary research in driving meaningful, data-oriented advancements across healthcare, sports, and biomedical fields.



AJITH ABRAHAM (Senior Member, IEEE) received the B.Tech. degree in electrical and electronic engineering from the University of Calicut, in 1990, the M.S. degree from Nanyang Technological University, Singapore, in 1998, and the Ph.D. degree in computer science from Monash University, Melbourne, Australia, in 2001.

He is currently the Vice Chancellor of Sai University, India. Prior to this, he was the Vice Chancellor of Bennett University, the Dean of the Faculty of Computing and Mathematical Sciences at FLAME University, Pune, and the Founding Director of Machine Intelligence Research Laboratories (MIR Labs), USA, a not-for-profit scientific network for innovation and research excellence that connects industry and academia. He has also held two university professorial appointments, including a Professor of artificial intelligence at Innopolis University, Russia, and the Yayasan Tun Ismail Mohamed Ali Professorial Chair of Artificial Intelligence at UCSI, Malaysia. He is involved in a multi-disciplinary environment and has authored or co-authored more than 1500 research publications, including over 100 books covering various aspects of computer science. One of his books was translated into Japanese, and several articles have been translated into Russian and Chinese. He has more than 61 000 academic citations, with an H-index of over 116 as per Google Scholar. He has given more than 250 plenary lectures and conference tutorials in over 20 countries.

Dr. Abraham served as the Chair for the IEEE Systems, Man, and Cybernetics Society Technical Committee on Soft Computing, which has more than 200 members, from 2008 to 2021. He was the Editor-in-Chief of *Engineering Applications of Artificial Intelligence* (EAAI), from 2016 to 2021, and has served on the editorial board for over 15 international journals indexed by Thomson ISI. Additionally, he was a Distinguished Lecturer of the IEEE Computer Society representing Europe, from 2011 to 2013.